ERDA/JPL 954373 - 77/6
Distribution Category UC-63

HEAT EXCHANGER-INGOT CASTING/SLICING PROCESS

Silicon Sheet Growth Development for the Large Area Silicon Sheet Task of the Low Cost Silicon Solar Array Project

Sixth Quarterly Progress Report
by
Frederick Schmid

Covering Period from December 17, 1976, to March 21, 1977
Date of Report: March 31, 1977

JPL Contract No. 954373

CRYSTAL SYSTEMS, INC.
35 Congress Street
P. O. Box 1057
Salem, MA 01970

This work was performed for the Jet Propulsion Laboratory, California Institute of Technology, under NASA Contract NAS7-100 for the U. S. Energy Research and Development Administration, Division of Solar Energy.

The JPL Low-Cost Silicon Solar Array Project is funded by ERDA and forms part of the ERDA Photovoltaic Conversion Program to initiate a major effort toward the development of low-cost solar arrays.

This report contains information prepared by Crystal Systems, Inc., under JPL subcontract. Its content is not necessarily endorsed by the Jet Propulsion Laboratory, California Institute of Technology, or the National Aeronautics and Space Administration, or the U.S. Energy Research and Development Administration, Division of Solar Energy.

MAN-HOURS AND COST TOTALS

Previous		Current		Cumulative	
M/Hr.	Cost	M/Hr.	Cost	M/Hr.	Cost
4,515	$206,459	1,959	$ 78,713	6,474	$285,172

TABLE OF CONTENTS

ABSTRACT

Efforts in crystal casting during this quarter were directed towards developing a crucible to prevent cracking and establish parameters for achieving the maximum growth rate for single crystal ingot solidification. Emphasis was placed on reducing the furnace superheat to increase growth rate and to cast SiO_2 liners directly in graphite crucibles.

Fast growth rates were achieved by reducing the furnace temperature as close to the melt point as the instrumentation would allow--3°C. Good single crystal growth was achieved on top of the seed by this technique, but the periphery of the seed was too cool to seed single crystal growth. Ingots were quenched from 1000°C with helium to shatter the crucible; this did not prevent cracking of the ingot. Low density fused silica bodies were fabricated. The wetting characteristics of liquid silicon in a vacuum atmosphere was sufficient to cause penetration into open paths such as cracks and voids.

Slicing tests were performed to determine: (1) the effectiveness of grooved support rollers in reducing blade wander, (2) the effectiveness of slow, non-synchronous and stationary workpiece motions on slicing

performance; and (3) the performance and life of diamond plated tungsten wire.

With grooved rollers positioned on either side of the workpiece, blade wander and wafer taper were reduced an order of magnitude. For a stationary workpiece, twice the blade force was required to obtain cutting rates comparable with rocked workpieces. This resulted in wire breakage, deterioration of cutting rate, and waviness of wafer surfaces.

Slow non-synchronous rocking of the workpiece dramatically improved the surface quality. Wafers could be sliced at 0.2 lb., 90 gm, instead of 0.15 lb., 68 gm, force per wire and still produce high surface quality.

Eighteen runs were conducted with the same 5 mil, 0.12 mm tungsten wires plated with 400 mesh diamonds. No wires or wafers were broken, and no significant deterioration of slicing performance or wafer quality was observed on any of the eighteen cuts through the 4 x 4 cm workpiece. The wafers from these tests are the highest quality to date.

SUMMARY AND PROGRESS

SILICON CRYSTAL CASTING

Efforts in crystal casting during February were directed towards developing a crucible and casting procedure to prevent cracking and establish parameters for achieving the maximum growth rate for single crystal ingot solidification. Emphasis was placed on reducing the furnace superheat to increase growth rate and to cast SiO_2 liners directly in graphite crucibles.

The operating parameters for runs 51 through 69-C are presented in Table I, Tabulation of Heat-Exchanger and Furnace Temperatures.

Establishing Parameters for Achieving Maximum Growth Rates

Previous reports have shown that growth rate is very sensitive to furnace temperature and rate of furnace temperature decrease. To achieve fast growth rates, the furnace temperature should be maintained as close to the silicon melt point as the instrumentation will allow. The heat exchanger temperature must be decreased rapidly to conduct away the heat of fusion and force the growth

TABLE I.

TABULATION OF HEAT-EXCHANGER AND FURNACE TEMPERATURES

RUN	PURPOSE	SEEDING		GROWTH CYCLE			REMARKS
				RATE OF DECREASE			
		FURN. TEMP. ABOVE M.P. °C	H.E. TEMP. BELOW M.P. °C	H.E. TEMP. °C/HR.	FURN. TEMP. °C/HR.	GROWTH TIME IN HOURS	
51	Determine maximum growth rate. Increase rate of heat exchanger temperature decrease.	11	1362	155	2.36	4.66	Seed melt out. Polycrystalline ingot.
52	Determine maximum growth rate and prevent cracking.	6	1360	111	1.2	5	Good seeding. Helium back filled at 840°C to break crucible. Ingot shattered.
53	Develop coating inside graphite crucible to prevent cracking.	4				1	No silicon penetration into crucible or cracking of silicon.
54	Develop coating inside graphite crucible to prevent cracking.	1				.1	Silicon penetrated graphite.
55	Develop coating for graphite and fused silica crucibles.	12		Terminated power.			Graphite crucible cracked due to penetration of silicon. Some cracking in fused silica crucibles.
56	Develop coating for fused silica crucibles to prevent cracking.	15				4	Silicon penetrated behind coating causing ingots to crack.

TABLE I. (Cont.)

TABULATION OF HEAT-EXCHANGER AND FURNACE TEMPERATURES

RUN	PURPOSE	SEEDING		GROWTH CYCLE			REMARKS
				RATE OF DECREASE			
		FURN. TEMP. ABOVE M.P. °C	H.E. TEMP. BELOW M.P. °C	H.E. TEMP. °C/HR.	FURN. TEMP. °C/HR.	GROWTH TIME IN HOURS	
57	Develop coating for graphite and fused silica crucibles.	5				.1	SiO coating evaporated allowing silicon to contact the fused silica crucible.
58	Develop coating for graphite and fused silica crucibles.	10				2	Coating failed. Silicon contacted surface.
59-C	Determine maximum growth rate and prevent cracking.	< 5	1382	84	1.43	3.5	Top froze over as ½" thick single crystal. Partial seed melt back and single growth from seed.
60-C	Determine maximum acrual growth rate. Graphite plate seated on heat exchanger to extract heat across entire bottom.	< 5	37 (1360)	81	3.14	3.5	Top froze as ½" thick polycrystalline layer. Good seeding with single crystal growth from seed.
61-C	Same as 60-C. Reduced heat loss by reducing size of view port in top cover.	< 6	21 (1383)	79	1.16	5.16	Good seeding and growth to top of ingot.

TABLE I. (Cont.)

TABULATION OF HEAT-EXCHANGER AND FURNACE TEMPERATURES

RUN	PURPOSE	SEEDING		GROWTH CYCLE			REMARKS
		FURN.TEMP. ABOVE M.P. °C	H.E.TEMP. BELOW M.P. °C	RATE OF DECREASE H.E. TEMP. °C/HR.	RATE OF DECREASE FURN. TEMP. °C/HR.	GROWTH TIME IN HOURS	
62-C	Same as 61-C. Thin wall crucible (.040")	< 5	21 (1384)	141	1.11	4.5	Silicon ingot shattered. Seed melt out.
63-C	Same as 60-C	Run terminated one hour after all liquid. Possible heat exchanger failure.					Polycrystalline material.
64-C	Develop liner inside graphite crucible to prevent cracking.	Approx. 15 (1.75 hr.)					Woven silica material failed. Second crucible--cast liner--silicon penetrated.
65-C	Grow single crystal to periphery of crucible and develop cooling cycle to prevent cracking.	< 5			1	3	Insufficient melt back on outer periphery of seed.
66-C	Develop crucible liner in graphite mold. Cycle quartz through high low transformation temperature.	Heat to 850°C in vacuum for two hours.					Low to high quartz transformation caused crucible to crack.
67-C	Grow single crystal	< 3	52 (1360)	80	0	4	Insufficient melt back on outer periphery of seed.

TABLE I. (Cont.)

TABULATION OF HEAT-EXCHANGER AND FURNACE TEMPERATURES

RUN	PURPOSE	SEEDING		GROWTH CYCLE			REMARKS
				RATE OF DECREASE			
		FURN. TEMP. ABOVE M.P. °C	H.E. TEMP. BELOW M.P. °C	H.E. TEMP. °C/HR.	FURN. TEMP. °C/HR.	GROWTH TIME IN HOURS	
68-C	Grow single crystal to periphery of crucible and develop cooling cycle to prevent cracking.	< 3	22	82	0	5	Insufficient melt back on outer periphery of seed.
69-C	Grow single crystal to periphery of crucible and develop cooling cycle to prevent cracking.	< 3	18	80	0	7	Insufficient melt back on periphery of seed.

interface to the ingot surface before the liquid is supercooled due to the decrease of the furnace temperature.

Runs 51, 52, and 59-C were undertaken to determine the maximum growth rate and to alter the cooling cycle to prevent cracking. By rapidly reducing the furnace temperature by quenching with helium, the outside surface cools and contracts more rapidly than the interior. It was hoped that the tension would cause the crucible to shatter before the ingot cracked.

In run 51 the instrumentation was not calibrated accurately allowing the furnace temperature to increase to 11°C above the melt point and melt out the seed. The ingot was polycrystalline but strongly directional grains were present.

For run 52 the melt was superheated 6°C and the heat exchanger was increased to 1360°C. After growth the ingot was cooled to 840°C in 20 hours. At this temperature the power was turned off and helium was backfilled into the furnace to a pressure slightly below atmospheric. The furnace was cooled to 575°C in approximately 2 hours at which time the ingot burst. The ingot shattered into many pieces. Sectioning showed that good seeding and single crystal growth had occurred.

For crystal casting run 59-C, the furnace was heated above the melt temperature until all the melt stock was melted. It was slowly decreased in temperature until the top froze over with a thin skin. The heat exchanger temperature was increased from 1280 to 1382°C and held at this temperature for one hour. The thin skin was still across the entire top of the melt when solidification was started by decreasing the furnace temperature 1.43°C per hour and the heat exchanger at 84°C per hour. After 3½ hours, the temperature monitored on the crucible wall declined rapidly indicating that solidification was complete.

For this run the furnace was cooled to 1022°C in 12 hours. The power was turned off and helium was backfilled into the furnace. The temperature was decreased to approximately 250°C in 3½ hours. Cracking was not observed with the fibre optic light source; however, the ingot was again shattered. Quenching with helium did not prevent cracking in the silicon ingot and does not appear to be a promising solution.

A polished and etched cross-section of boule 59-C is shown in Figure 1, Polished and Etched Cross-Section of Boule 59, 60, 61, and 62. Figure 1 shows that seed melt back was not complete near the top and outer periphery, but single crystal growth was good in the

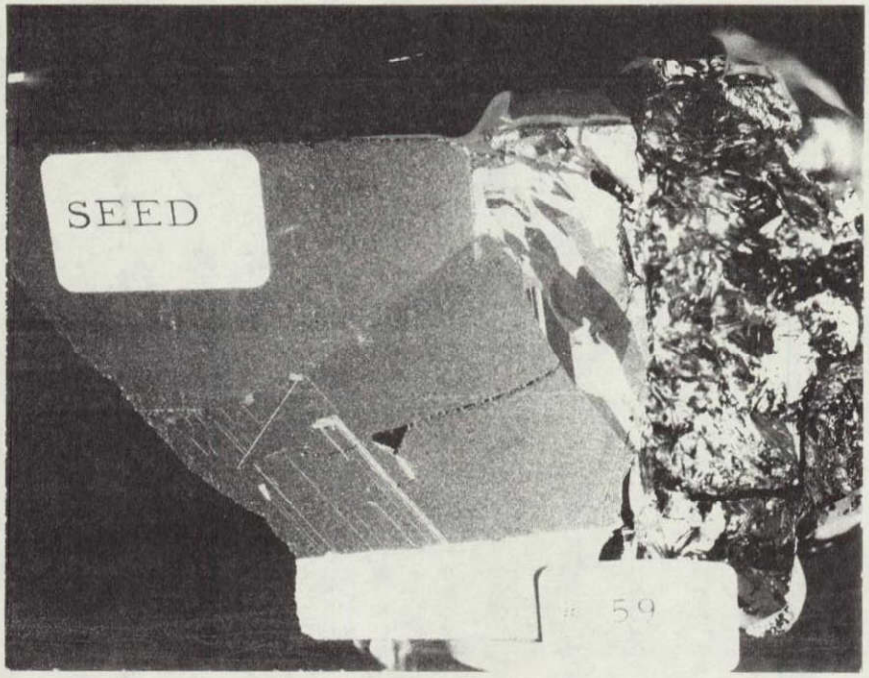

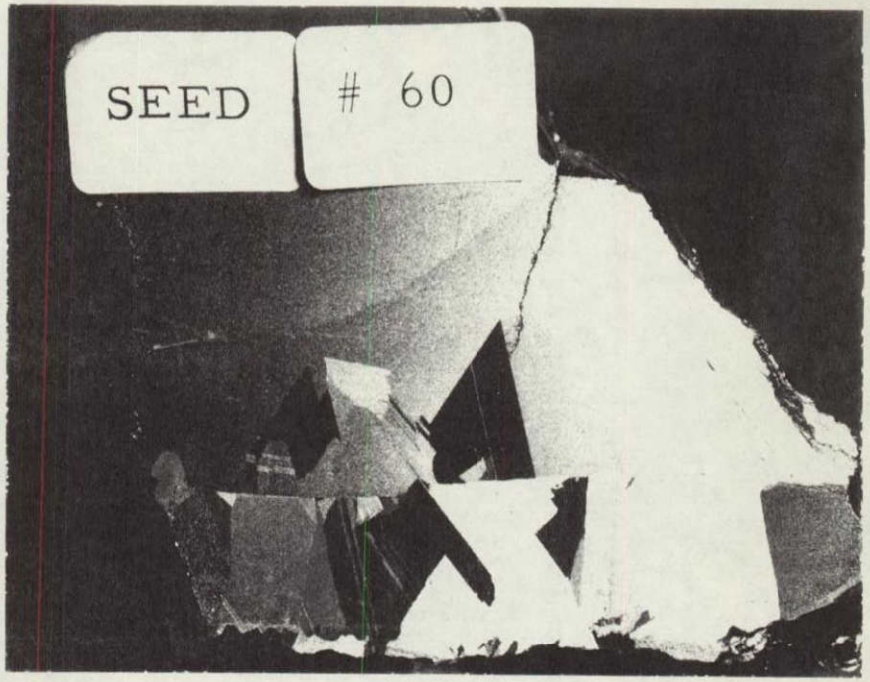

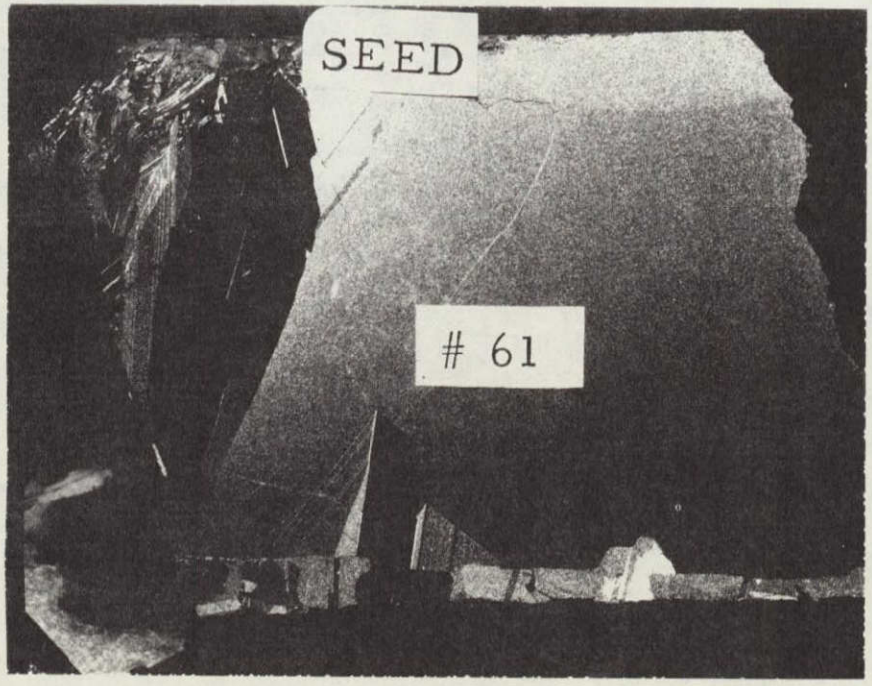

Figure 1. Polished and Etched Cross-section of Boules 59-C, 60-C, 61-C, and 62-C.

central section of the ingot. The entire top of the ingot which appeared as a white area in Figure 1 was single crystalline, apparently nucleated from the thin skin that formed on top at the start of solidification. As the furnace temperature was decreased, single crystal material grew down into the melt. It grew one-half inch down into the melt before it made contact with the single crystal growing up from the bottom. From this run it is apparent that the temperature at the top of the melt is cooler than at the bottom. The shape of the seed gives one a good perspective of the shape of the isotherm at the beginning of solidification.

For run 60-C the heat flow conditions were changed by seating a graphite disc on the heat exchanger. The crucible is positioned directly on this plate to increase the seed temperature during seeding to assure sufficient seed melt back. During growth the plate can conduct heat from the bottom of the crucible to the heat exchanger.

As for run 59-C, the furnace temperature was decreased until a solid skin grew over the entire top of the melt. The heat exchanger temperature was only increased to 1362°C, 20°C lower than for run 59-C, and the furnace temperature decrease was increased from 1.43 to 3.14°C per hour. After 3½ hours' growth, the crucible

broke due to entrapment of liquid between the growth from the top and growth from the seed. Figure 1 shows that good seed melt back and seeding was achieved. Crystal growth was not particularly good as evidenced by grains above the seed.

It appeared that seeding was improved by the graphite plate but growth problems were created either due to the graphite plate or due to the increased rate of temperature decrease of the melt.

Figure 1 shows clearly that the top of the melt is cooler than the bottom causing solidification to progress from the top and bottom towards the center. One source of heat loss from the top center of the heat zone is the 2" diameter viewing port. This was insulated and closed to one-half inch for run 61-C to minimize heat loss from the top center of the furnace.

It is apparent from Figure 1 that the seed should be melted back more. Therefore the heat exchanger temperature was increased to 1382^{o}C and furnace temperature increased approximately 1^{o}C above the previous run. No skin formed over the melt. The rate of furnace temperature decrease was slowed to 1.16^{o}C per hour. This caused the growth time to increase from 3.5 to 5.16 hours.

Both seeding and growth were improved over the

previous two runs as can be seen in Figure 1. The seed was melted back substantially in the vertical dimension but only slightly on the diameter. Single crystal growth was almost complete to the top of the melt.

For run 62-C the furnace temperature was decreased 1°C from the previous run but the seed melted out probably during the heat-up cycle. For this run, a 1 mm wall thickness crucible was used so the crucible would break before the ingot broke. The ingot was polycrystalline and cracked into small pieces as is apparent in Figure 1, a polished and etched cross-section of run 62-C. Run 63-C had to be terminated due to a heat exchanger failure one hour after the silicon was melted.

Run 65-C was a repeat of run 63-C but the furnace temperature was held at approximately 4°C above the melt point and decreased at 1°C per hour during growth. The thermocouple in the heat exchanger failed during seeding. It was estimated that the temperature was about 1362°C and was decreased at 80°C per hour. The ingot was solidified in three hours. It was apparent from fractured sections of the ingot that the seed had melted out. Apparently the heat exchanger temperature was higher than our estimates causing seed melt out.

For run 67-C the furnace temperature was held less than 3°C above the melt point and the heat exchanger

temperature was held at 1360°C. Since the furnace temperature was only 3°C above the melt point, the furnace temperature was not decreased but only the heat exchanger temperature was decreased at 80°C an hour. It required four hours for complete solidification even though the furnace was about 3°C above the melt point. Solidification occurred from the top down into the melt and from the seed up. Good seed melt back occurred except the outer periphery of the seed that was in contact with the crucible. Single crystal growth occurred above the seed to within 1 cm from the top where it contacted the layer growing down from the top. Single crystal growth broke down from the edge of the seed where there was almost no melt back. It appears that the bottom of the crucible near the outer periphery of the seed was too cool and therefore, there was no seed melt back and seeding.

In view of this problem, heat flow conditions on the bottom of the crucible were changed. A 2 cm thick graphite plate was placed under the crucible to conduct more heat to the bottom center of the crucible. For this run the furnace temperature was again held at less than 3°C above the melt temperature, but the heat exchanger temperature was allowed to increase to 1390°C in order to melt back the periphery of the seed.

The melt was doped with boron to achieve a resistivity of approximately 5 Ω cm.

After solidification was complete the heat exchanger temperature was 955°C. For this boule, the heat exchanger temperature was not increased to equilibriate the temperature of the boule but instead the furnace temperature was lowered while the heat exchanger was held constant at 955°C.

This cycle would minimize the effects of the expansion mismatch of the silicon and silica. Silicon in contact with the crucible wall is prevented from contracting during cool down since the center section is held constant at 955°C. The temperature of the boule was then reduced from 955°C to room temperature in about 15 hours. This procedure reduced the cracking but did not eliminate it. A polished cross-section Sirtl etched revealed that the outer periphery of the seed was not melted back. The outer periphery of the seed is approximately 1 cm high. Above this height, the seed melted back in the form of a hemisphere and single crystal growth occurred. Single crystal growth did not occur from the bottom edge of the seed where it was too cool for melt back to occur. The resistivity ranged from 2 to 8 Ω cm in the central single crystal region.

Run 69-C was the same as for 68-C, but the furnace temperature was increased by approximately 1°C to achieve melt back on the bottom periphery of the seed. The cooling cycle was also identical except that the heat exchanger temperature was reduced to 775°C and held constant during cool down. The cooling cycle minimized but did not prevent cracking. A fracture cross-section through the seed shows that melt back was not achieved on the outer periphery of the seed. The boule is currently being sectioned for further characterization.

In conjunction with the experimental work described above, an equipment design was started to monitor the position of the interface with ultrasonics.

Development of a Crucible to Prevent Cracking

Runs 53, 54, 55, 56, 58, and 64-C were conducted to develop coatings or crucibles that would prevent cracking of the crucibles and ingots. Previously it was shown that silica coatings on fused silica crucibles can prevent cracking. Ingot cracking only occurred when the coating allowed silicon to contact the clear fused silica crucible.

Runs 54, 55, 56, 57, and 58 were performed to evaluate various grain size fused silica coatings on

clear fused silica crucibles.

Run 54 was spray-coated with 1 part 200-mesh fused silica powder and 3 parts coloidal silica binder. It was sintered for 16 hours at 500°C, loaded with 30 gm silicon, and heated above the silicon melt point. The run was terminated after six minutes due to silicon penetration onto a graphite crucible that was run along with this run. The coating failed on the fused silica crucible causing areas of the ingot to crack. Silicon penetrated a crack or weak spot in the coating to contact the clear fused silica wall.

For run 55, 30 ml fused silica crucibles were rough ground inside and etched with 50% HF for 30 minutes. The crucibles were spray coated with a mixture consisting of 3 parts coloidal silica binder and 1 part 80/200 mesh fused silica powder. 80/200 mesh powder is screened through 80 mesh screen onto a 200 mesh screen; therefore, the grain size is no larger than 177 or smaller than 74 microns. After sintering at 500°C for four hours, the crucibles were loaded with 35 grams of silicon and heated above the melt point. Areas of the ingots cracked when silicon penetrated breaks in the silica coating.

Run 56 was conducted the same as run 55, but with a 140 mesh fused silica powder. The coating failed in certain areas due to poor bonding to the surface of the

fused silica crucible.

From the previous two runs it appeared that the coarse particles did not bond to the crucible sufficently, allowing molten silicon to lift the coating and bond to the wall. Therefore 200 mesh silica particles were used for two 30 ml fused quartz crucibles used in run 58.

An unground crucible was spray-coated with 200 mesh fused silica sintered at 460°C for 12 hours, re-spray-coated, and sintered at 460°C for one hour. A second 30 ml crucible that had been abraded on the inside surface was spray-coated with 200 mesh alpha quartz and sintered at 200°C for one hour. The crucibles were loaded with 35 gms of silicon heated 10°C above the silicon melt point for two hours and cooled to room temperature. The quartz-coated crucible shattered and the upper portion of the ingot cracked. The fused silica crucible remained intact but was cracked. Fine cracks were induced in the top edge of the silicon ingot. Failure of the spray coatings appears to be due to weak bonding between the coating and crucible. When the coating separates from the crucible wall, molten silicon breaks through and adheres to the wall causing the crucible and ingot to crack on cool down.

Cracking can be prevented by coating fused silica crucibles, but this may not be the most economical or

reliable crucible. Graphite crucibles coated or lined with fused silica would be more economical if the graphite mold could be reused many times. Graphite's expansion coefficient of approximately 4 x 10^{-6}cm/cm^{o}C is close to silicon's expansion coefficient and therefore will not induce cracking in the silicon ingot or crucible. In light of this, silica lining for graphite crucibles was studied. A graphite crucible was spray coated with 200 mesh fused silica dried at 300^{o}C for one half hour, loaded with 20 gm of silicon and heated 4^{o}C above the melt point for one hour. The coating blistered in several areas. The silicon in the bottom was not cracked, since the silica coating prevented silicon from penetrating into the crucible.

A pyrolytic coated graphite crucible was spray-coated with fused silica and tested as described earlier for run 54. Silicon penetrated through the silica coating, pyrolytic coating, and graphite crucible to form SiC causing the crucible to break. In run 55, a graphite crucible was spray coated as described for run 54. This coating failed and the power had to be terminated. Failure of the fused silica coatings on the graphite crucibles appears to be due to the large difference in the expansion coefficients of graphite (approximately 4 x 10^{-6}cm/cm^{o}C) and fused silica (.5 x 10^{-6}cm/cm^{o}C). The graphite

expands away from the silica coating due to its higher coefficient of thermal expansion. Spray coatings are thin, and when unsupported by the graphite, break, allowing the silicon to penetrate into the graphite.

One difficulty associated with developing reliable coatings for silica or graphite crucibles may be shrinkage associated with sintering. As the coating shrinks, it is put into tension. This causes cracks to develop allowing silicon to penetrate the crack and lift the coating. It would be desirable to put the coating into compression to prevent cracks from forming.

It appears that graphite crucibles must be coated with SiO_2 that has an expansion coefficient as large as or larger than the graphite. Crystalline quartz has an expansion coefficient of approximately 7×10^{-6} cm/cm^{o}C and undergoes an expansive transformation at 573^{o}C, making it a particularly attractive coating for graphite crucibles.

The relationship of fused silica to its crystalline counterparts is often a source of confusion. Fused silica is a noncrystalline form of silicon dioxide. Essentially, it is a high-viscosity melt phase, or glass, that is thermodynamically unstable, but kinetically stable at ordinary temperatures. At atmospheric pressure, the crystalline forms of silica are quartz, tridymite, and cristobalite. The densities of these polymorphic forms

are 2.65, 2.26, and 2.33 g/cm^3, respectively, whereas the density of fused silica is 2.20 g/cm^3.

Quartz is the stable crystalline form from room temperature up to 1140°K. Tridymite is stable from 1140°K to 1743°K, and cristobalite is stable from 1743°K up to its melting point, 1996°K. Each of these, in turn, has additional polymorphic forms within different temperature ranges.

Tridymite is particularly interesting since it is the stable equilibrium phase in the temperature range of interest, its coefficient of thermal expansion is close to both silicon and graphite, and it only undergoes a small volume change during the displacive transformation at 160°C.

Silicon reacted with fused silica above 500°C in vacuum will form silicon monoxide:

2.2 g/cc		2.33 g/cc		2.05 g/cc
SiO_2	+	Si	→	2 SiO

Silicon monoxide is unstable at 1412°C in .1 Torr pressure, but it could be protected by a protective layer of SiO_2. This approach was used in run 57 using a 30 ml clear fused quartz crucible and a graphite crucible. The crucibles were spray-coated twice. The first coating was 1 part 100 mesh silicon, 1 part 200 mesh silica and 6 parts coloidal silica binder. After heating to 200°C for 3½ hours, a second coating consis-

ting of 1 part 200 mesh fused silica and 3 parts coloidal binder was applied. After sintering at 200°C for four hours, the crucibles were loaded with 35 gms of silicon and heated above 1412°C for six minutes. Considerable outgassing was experienced as the silicon melted, since it penetrated the coating and reacted with graphite to form SiO. The ingots and crucibles from this run were completely shattered. It is apparent that the second coating of SiO_2 did not prevent the SiO from evaporating.

For run 58 coatings were made starting with quartz powder, since theoretically the quartz should undergo an expansive transformation to form tridymite. This may compensate for sintering shrinkage that causes failure. A graphite and 30 ml fused silica crucible were spray-coated with 200 mesh alpha crystalline quartz powder. A slurry of 3 parts binder and 1 part powder did not spray-coat easily; therefore, non-uniform coatings were developed. After drying the coatings at 200°C for 2 hours, the crucibles were loaded with 30 gms of silicon, heated 10°C above the melt point for two hours, and cooled to room temperature. The fused silica crucible shattered since liquid silicon had penetrated under the coating. Possibly the expansive transformation and high expansion coefficient of approximately 7×10^{-6} cm/cm°C caused the coating to buckle off the fused silica.

For the graphite crucible, there was almost no trace of the coating on the wall. Silicon ran to the outer periphery of the crucible bottom, but did not penetrate or crack either the crucible or thin section of silica. The thin coating did not adhere to the crucible, and was probably unable to support itself. Traces of the coating were observed on the bottom. Debye-Sherrer x-ray diffraction patterns were made from quartz coatings that were heated above the melting point of silicon. The patterns contained few quartz liners but strong tridymite and cristobalite patterns. The quartz apparently transformed to a distorted cristobalite phase as suggested by Coyle.[1]

The graphite crucible spray coated with crystalline quartz failed probably because it was not thick enough to resist buckling.

Thicker liners appear more reliable because they can be fabricated more reproducibly and are thicker, therefore stronger. Liners can be fabricated by slip casting or by casting directly in a graphite crucible. AVCO's Materials Division has contracted to slip cast fused silica and crystalline quartz liners.

In addition, some commercially available slip cast fused silica crucibles are on order and will be evaluated. It has been shown in the JPL wetting study that the slip cast fused silica caused very little cracking of the silicon

in contact with it. This supports our observations that sintered coating prevents cracking of the silicon ingots. Bonded fused silica particles are not strong enough to break the silicon ingot. Crucibles fabricated out of tridymite might be the ideal solution, since the coefficient of thermal expansion of tridymite is close to silicon and graphite. No stress would be induced on the ingot surface for it would not have to tear free of the crucible.

Casting a liner directly in a graphite crucible appears to have economic and technological advantages over slip casting and therefore it is being pursued. Basically, this process involves pouring a slurry into a graphite crucible and extruding it up the sides of the crucible with a mandrel. The mandrel describes the shape of the crucible interior and is removed when the lining is dry.

A slurry with approximately 70%, 325-mesh crystalline quartz and 30% binder was poured into a graphite crucible and a .100 wall thickness liner was extruded with a mandrel. There was considerable porosity in the coating. The crucible and liner were baked out on a hot plate at 80°C for several hours. Before loading in the furnace, several pieces of silicon were placed in this crucible so they could be observed when they melted. A small graphite crucible lined with a fused silica blanket and

loaded with a small piece of silicon was also loaded into the furnace. The furnace was evacuated and heated to 1400°C in 16 hours. The temperature was increased to 1418°C and liquid was observed after two hours. It was held at this temperature for 1½ hours before the power was turned off.

There was no sign of reaction between the quartz liner and the silicon. Silicon penetrated into the pores, but not into the graphite, and the silicon layer on the bottom of the crucible was not cracked. Debye-Scherrer x-ray diffraction patterns were made from the quartz liner. The quartz has transformed to a distorted cristobalite.

The silicon in the other crucible penetrated through the fused silica blanket and cracked the crucible due to SiC formation. The wetting characteristic of silicon in vacuum appears to be sufficient to cause silicon to penetrate into open porosity or voids.

It appears that coatings and liners will have to be dense with no interconnecting porosity since the silicon will penetrate through any open path in the silica. In view of this it is apparent that high density crack-free liners are required. To achieve high density by slip casting, small-size continuous particle distribution (less than 10 micro meter) is required. A continuous

particle size distribution is achieved by ball milling, but air is also incorporated into the slip due to the rolling action. The air can be removed by evacuating the contents under a mechanical pump vacuum.

Shrinkage occurs during drying of the slip. Cracking can occur if the rate of drying is not carefully controlled. The overall shrinkage can be controlled by controlling the initial water content. A certain amount of drying shrinkage is associated with thickness of the water film between particles. By decreasing the thickness of the water film, the over-all drying shrinkage is reduced. The solids content can be as high as 83%. Unfortunately, the water content cannot be reduced below this level or the slip will not flow.

Crystal Systems has developed a pressure casting technique where the slip is pressure cast in a graphite mold to force the particles together and force the water into the mold. This method minimizes shrinkage.

A 325 mesh quartz slip was prepared and evacuated with a mechanical pump for run 66-C. Two liners were slip cast in graphite crucibles. One liner was made using 30% DI water and the other using 30% coloidal silica binder. The crucibles were heated up to 850^{o}C for two hours in vacuum to determine the degree of sintering shrinkage and to determine the effect of the high-low

quartz displacive transformation. There was no evidence of sintering or shrinkage in the crucible liner made with water. The liner made with the coloidal silica binder expanded sufficiently during the low to high transformation to cause the crucible to crack. It appears that the bond between the particles was too strong to allow for rearrangement during the expansion that occurred during the transformation. On the other hand, the quartz particles in the liner made with no binder were not bonded and rearranged to allow for expansion.

It appears that the quartz expands more than enough to make up for the sintering shrinkage. To allow for particle rearrangement during sintering, the amount of coloidal binder will have to be reduced to decrease its strength. Alternatively, the quartz powder can be heat-treated to form tridymite before it is made into a slip.

DERIVATION OF THE MAXIMUM THEORETICAL GROWTH RATE

In deriving the equation for the maximum growth rate, it is assumed that the interface is hemispherical as shown in Figure 2, Schematic of Crystal Growing Furnace. The symbols and constants are identified in Figure 3, Identification of Symbols, and the Temperature of the Heat Exchanger and Helium Inlet and Exhaust Temperature vs. Helium Flow Rate is presented in Figure 4.

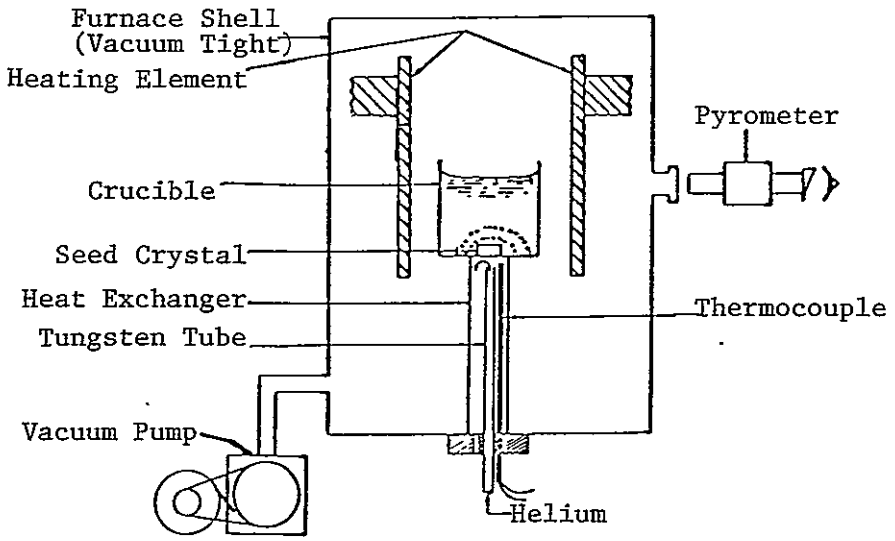

Figure 2. Schematic of Crystal Growing Furnace

Heat Flow for the Heat Exchanger Method is as follows:

Latent Heat + Heat In = Heat Out

(1) $L \frac{dm}{dt} + A_l K_l \frac{dT}{dr_l} = A_s K_s \frac{dT}{dr_s}$

(2) $\frac{dm}{dt} = 2\pi r^2 \rho_s \frac{dr}{dt}$ assuming hemispherical growth interface

(3) $2\pi r^2 L \rho_s \frac{dr}{dt} + 2\pi r^2 \frac{dT}{dr_l} = 2\pi r^2 K_s \frac{dT}{dr_s}$

(4) $\frac{dr}{dt} = \frac{K_s \frac{dT}{dr_s} - K_l \frac{dT}{dr_l}}{\rho_s L}$

(5) Maximum Growth Rate $\frac{dr}{dt} = \frac{K_s \frac{dT}{dr_s}}{\rho_s L}$

(6) $2\pi r_s^2 K_s \frac{dT}{dr_s} = C_p Q (\Delta T)$ heat removed by helium gas

(7) Maximum Growth Rate $\frac{dr}{dt} = \frac{C_p Q (\Delta T)}{2\pi r_s^2 \rho_s L}$

$$\frac{dr}{dt} = \frac{.2215 \text{ Cal}/_{1^oC} (\Delta T^oC) \quad Q \text{ 1/min}}{r^2 cm^2 \times 2\pi \times 432 \text{ Cal}/_{g} \times 2.3 g/_{cm^3}}$$

$$\frac{dr}{dt} = \frac{3.54 \times 10^{-5} Q (\Delta T)}{r^2}$$

Determine maximum growth rate assuming:

$\Delta T \approx 1000^{o}C$ at 100 $^{l}/_{min}$ (Figure 4)

$Q = 100$ liter/min

$r = 4$ cm

$$\frac{dr}{dt} = \frac{3.5}{16} = .218 \text{ cm/min}$$

The preceding derivation and example shows that the maximum growth rate is dependent on the helium flow rate. To maintain growth rate constant, the helium flow must be increased as a function of r^2.

There is no theoretical maximum growth rate based on heat flow considerations. Growth rate is limited by the practical consideration of how large a gradient can be applied to the solid before it shatters.

L = latent heat of fusion - 432 Cal/g

T = temperature

K_l = thermal conductivity of the liquid

dT/dr_l = thermal gradient in the liquid at some point r_l close to the interface

A_l = $2\pi r^2$ = area of the isotherm which goes through r_l - assume = to areas of interface

k_s = thermal conductivity of the solid

dT/dr_s = thermal gradient in the solid near the interface

A_s = $2\pi r^2$ = area of the interface

ρ_s = density of the solid at M.P. 2.3 g/cm^2

dr/dt = radial growth rate

m = $2/3\pi r^3 \rho_s$

dm/dt = mass freezing per unit time = $2\pi r^2 \rho_s \frac{dr}{dt}$

C = Specific heat of helium 1.252 Cal/g^oC

(density of helium 0.1769 g/liter)

C = .2215 Cal/liter ^oC

Q = Flow rate - liter/min

Figure 3. Identification of Symbols

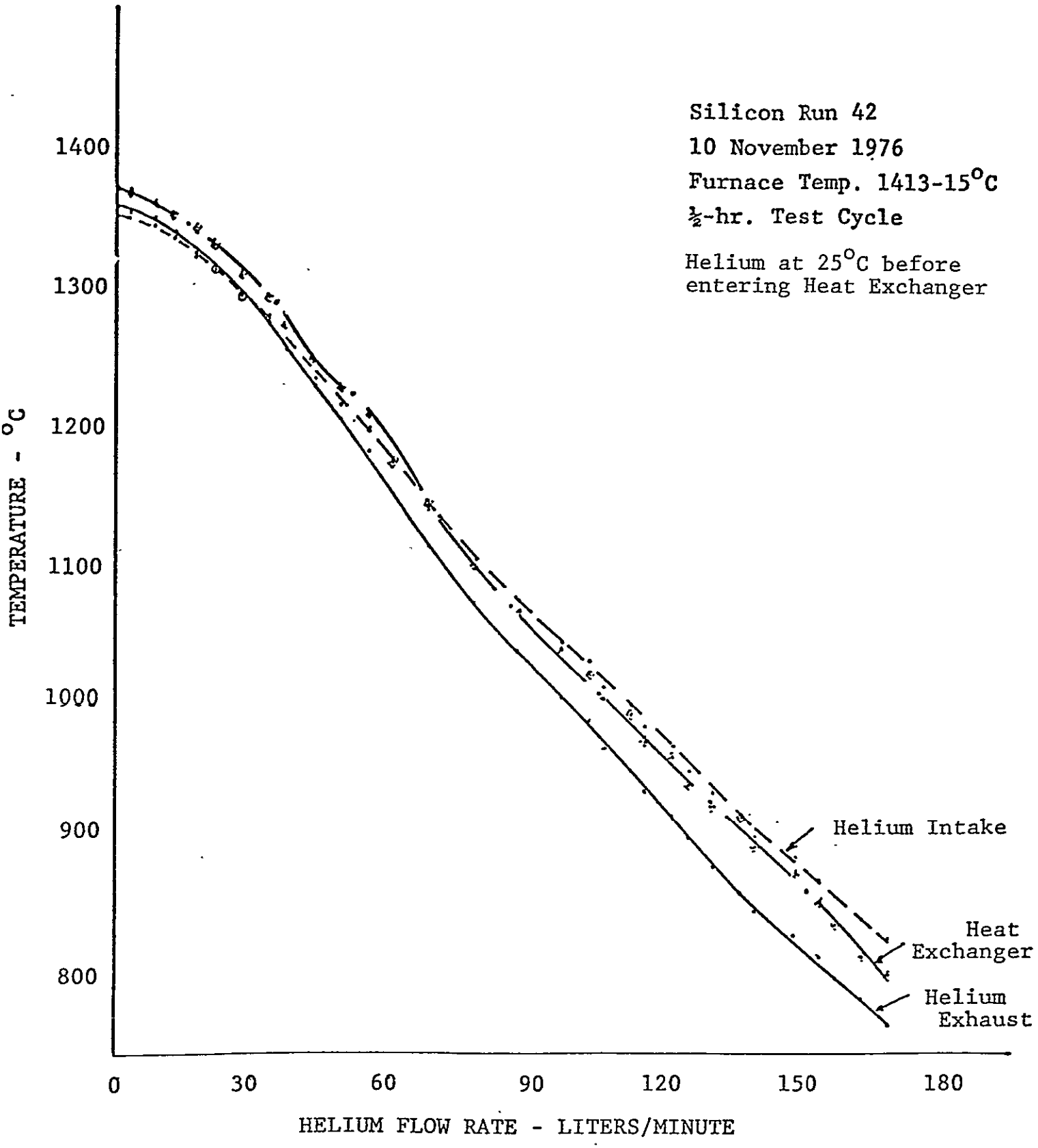

Figure 4.

Temperature of the Heat Exchanger and Helium Inlet and Exhaust Temperature vs. Helium Flow Rate

SILICON INGOT SLICING

Efforts in crystal slicing were concentrated on slicing silicon. Testing was directed toward the problems of wander, wafer surface quality, and blade life.

In conjunction with the slicing tests, wire and wafer characterization was conducted and the feed mechanism was modified to make it more rigid.

A summary of the cutting tests is presented in Table II. All slicing tests were performed on 3.8 cm (111) silicon cubes using 25 to 28 wires supported by grooved rollers on either side of the workpiece.

Run 12 was intended to measure the effect on blade wander with grooved blade support rollers positioned on either side of the workpiece.

Twenty-five blades were used, made from 6 mil, .15 mm stainless steel wire, coated with a 1 mil, .025 mm thick copper coating and charged two times with 45 μm natural diamonds.

During the run the machine was shut down for five days while modifications to the blade supports were made. In addition, prior to the shutdown, the water and detergent 60:1 coolant used in runs 10, 11, and the beginning of 12 was replaced with a water and Rust-Lick

TABLE II.

SILICON SLICING SUMMARY

RUN	PURPOSE	FEED FORCE/BLADE lb	gm	AVERAGE CUTTING RATE mil/min	mm/min	WIRE TYPE	REMARKS
12	Measure effects of blade wander with support rollers in position.	.15	68	1.5	.038	Double impregnated 45 μm diamond in copper plated .2 mm Ø wire	Run aborted midway due to low cutting rates.
13	Continuation of run 12 with new wires.	.15 .20	68 90	1.5 2-3	.038 .07	Double impregnated 45 μm diamond in copper plated .2 mm Ø wire	Rollers show significant improvement in blade wander. Damage at wire pack change.
14	Test Nickel-Diamond plated stainless steel wires.	.15	68	2.0	.05	400-mesh diamond nickel plated on .2 mm Ø stainless steel wire	Wire breakage due to hydrogen embrittlement.
15	Test cutting dry.					Double impregnated 45 μm diamond in copper plated .2 mm Ø wire	Loading observed. Further testing necessary.
16	Test run without rocking workpiece.	.3	136	2-2.5	.05	Double impregnated 45 μm diamond in copper plated .2 mm Ø wire	Twice normal feed forces were required to achieve usual cutting rates. Wafer surface quality poor.
17	Test effects of slow non-synchronous rocking of workpiece ½ cycle/minute.	.2	90	2-3	.06	Double impregnated 45 μm diamond in copper plated .2 mm Ø wire.	Very good surface quality and good cutting rates maintained throughout run.

TABLE II. (CONT.)

SILICON SLICING SUMMARY

RUN	PURPOSE	FEED FORCE/BLADE lb	gm	AVERAGE CUTTING RATE mil/min	mm/min	WIRE TYPE	REMARKS
18-S	First run using DiNi plated tungsten.	.2	90	6.6	.17	400 mesh diamond nickel plated on .127 mm tungsten wire	Cutting rates dropped to 2.5 mils/min at the end of this run.
19-S	Determine cause of cutting rate decrease.	.2	90	2.5	.06	Same wire.	This run was aborted midway through due to low cutting rates.
20-S	Wires used in runs 18-S and 19-S turned upside down.	.2	90	5.9	.15	Same wire.	Good cutting rates until contact was made with glass mounting block, again dropping to 2.0 mil/min.
21-S	Isolate cause of cutting rate decrease at completion of runs. Change mounting block to graphite.	.2	90	2.75	.07	Same wire.	Wire dressing with an aluminum oxide dressing stick. Cutting rates increased and also increased with contact in graphite.
22-S	Life test of wires and effects of dressing.	.2	90	3.9	.10	Same wire.	Good cutting rates and wafer quality.
23-S	Life test.	.2	90	4.1	.10	Same wire.	Light dressing prior to run.
24-S	Life test.	.2	90	3.5	.09	Same wire.	Slight decrease in cutting rates.
25-S	Life test.	.2	90	3.7	.09	Same wire.	Cutting rate seems to be stabilizing.

TABLE II (CONT.)

SILICON SLICING SUMMARY

RUN	PURPOSE	FEED FORCE/BLADE lb	gm	AVERAGE CUTTING RATE mil/min	mm/min	WIRE TYPE	REMARKS
26-S	Life test.	.2	90	3.6	.09	Same wire.	Amount of dressing and feed force are critical.
27-S	Life test.	.2	90	3.7	.09	Same wire.	Wafer thickness may be changing due to support roller degradation.
28-S	Life test.	.2	90	3.6	.09	Same wire.	Very good wafer surface quality. No dressing prior to this run.
29-S	Life test.	.2	90	3.7	.09	Same wire.	Same as run 28-S.
30-S	Life test and test effects of machine modifications.	.2	90	3.0	.08	Same wire.	Stiffening feed mechanism has improved wafer quality. Final feed calibration not complete at this time which may account for decreased cutting rates.
31-S	Life test; increase rate of rocking.					Same wire.	Calibration problem. Changed gear motor on rocking drive to 3.0 cycles/min.
32-S	Test effects of rocking 6 cycles/min	.2	90	4.2	.1	Same wire.	No pressure change during run. Improved surface quality.

TABLE II. (CONT.)

SILICON SLICING SUMMARY

RUN	PURPOSE	FEED FORCE/BLADE lb	gm	AVERAGE CUTTING RATE mil/min	mm/min	WIRE TYPE	REMARKS
33-S	Test effects of changing bladehead speeds at ten minute intervals	.2	90	3.76	.094	Same wire.	Steady increase in cutting rates with speed increases and steady increase in machine noise 80-100 cycles/minute test range.
34-S	Test effects of slow bladehead half usual speed 10 cycles/minute	.2	90	2.2	.06	Same wire.	No significant improvement in wafer surface quality.
35-S	Determine optimum rocking speed	.2	90	3.2	.08	Same wire.	Small hydraulic lines on rocking slave changed to accommodate faster speeds which changed calibration leaving feed force unknown
36-S	Test effects of dry cutting	.2	90	3.76	.1	Same wire.	Dry cutting was aborted due to a loading condition. Run continued wet with good cutting rates. No damage to wires from cutting dry.

40:1 coolant.

Cutting rates throughout testing remained in the 1 to 2 mil/min, .025 to .05 mm/min range at a blade force of 0.15 pounds, 68 gms, per blade. Slicing was interrupted for inspection of blades after one-half inch of cutting, when cutting rate remained approximately 1 mil/min.

Run 13

Run 13 was a continuation of the cut begun in run 12 using a second set of wire blades from the same lot of blade materials used in run 12. The coolant was an ethylene glycol and water 1:1 solution as used in runs 1 through 9.

Cutting rates, at a blade force of 0.15 pounds per blade, were in the 1 to 2 mil/min, .025 to .05 mm/min range as in run 12. An increase to 0.20 pounds, 90 gms, per blade resulted in an increase in cutting rate to the 2 to 3 mil/min, .05 to .075 mm/min range. Including the possible effects of a shutdown from Friday afternoon to Monday morning the cut was completed at a cutting rate of 2 mil/min, .05 mm/min, which was holding steady at the end of the run.

After slicing through the silicon block, a wire was examined with a SEM. SEM photographs showing the diamond

concentration and distribution and size are presented in Figure 5, SEM of 8 mil, .2 mm Copper Plated Stainless Steel Wire Impregnated with 45 μm Diamond Used in Run 13 (300X and 2000X).

It is interesting to note that there was no observable damage to the wire such as diamond pull out or wear on the copper plating. The cross-section illustrates the low diamond concentration.

Wafer surface quality during periods of continuous cutting was very good, with no scoring and almost no visible waviness. Damage occurred where the blade set was replaced after run 12.

The preliminary data currently suggests that taper ranges from 0.5 to 1 mil, .0127 to .025 mm over a 1", 2.5 cm depth of cut. Because of the limits of the current taper measuring process, the meaning of these values over a 4 inch, 10 cm depth of cut is presently unclear.

It does appear certain, however, that the use of support rollers has been an important addition to the process.

Run 14

In run 14, for comparison with the slicing performance of diamond-impregnated wire blades, a set of 27 diamond-plated stainless steel wire blades were used.

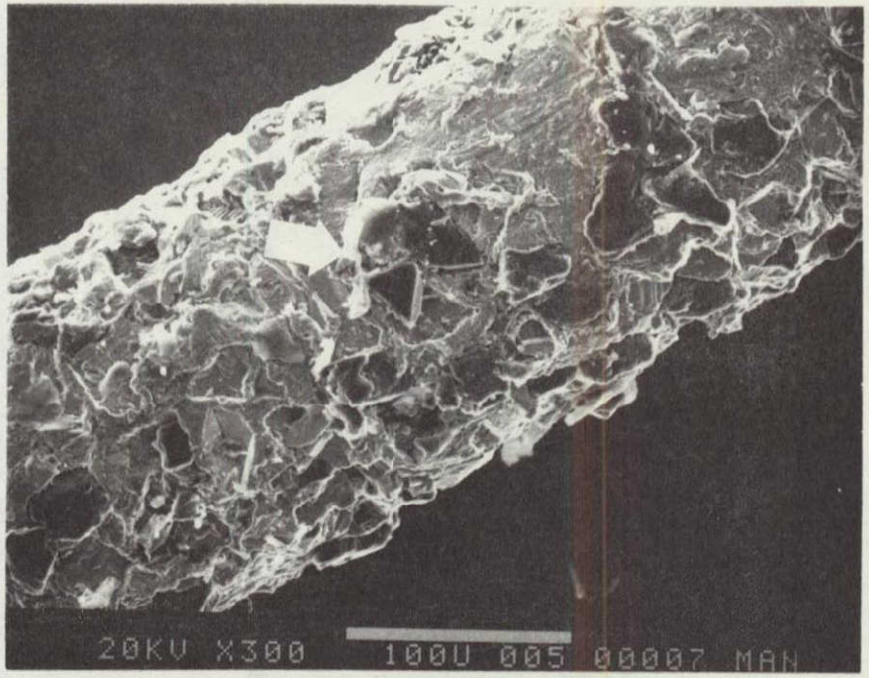

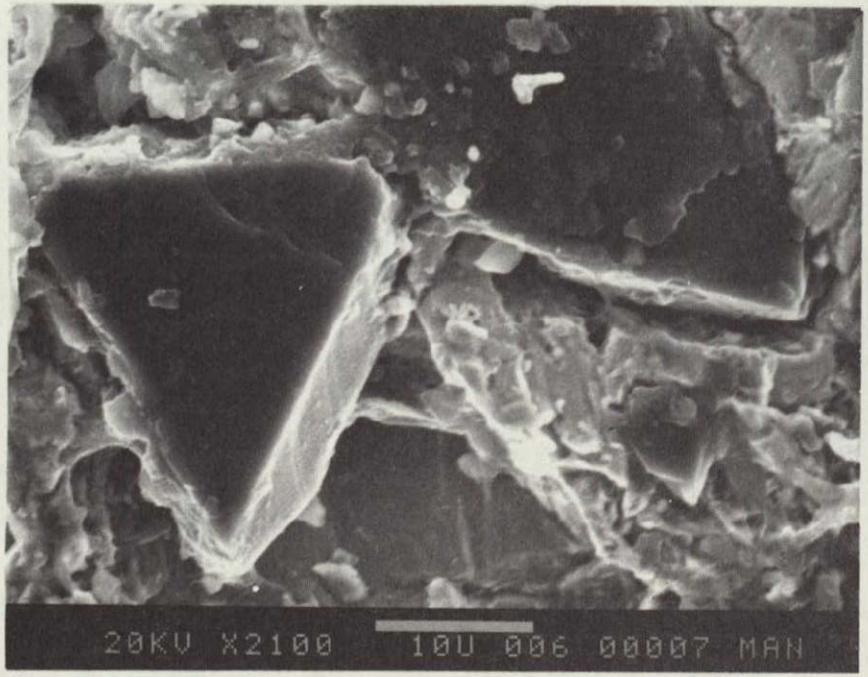

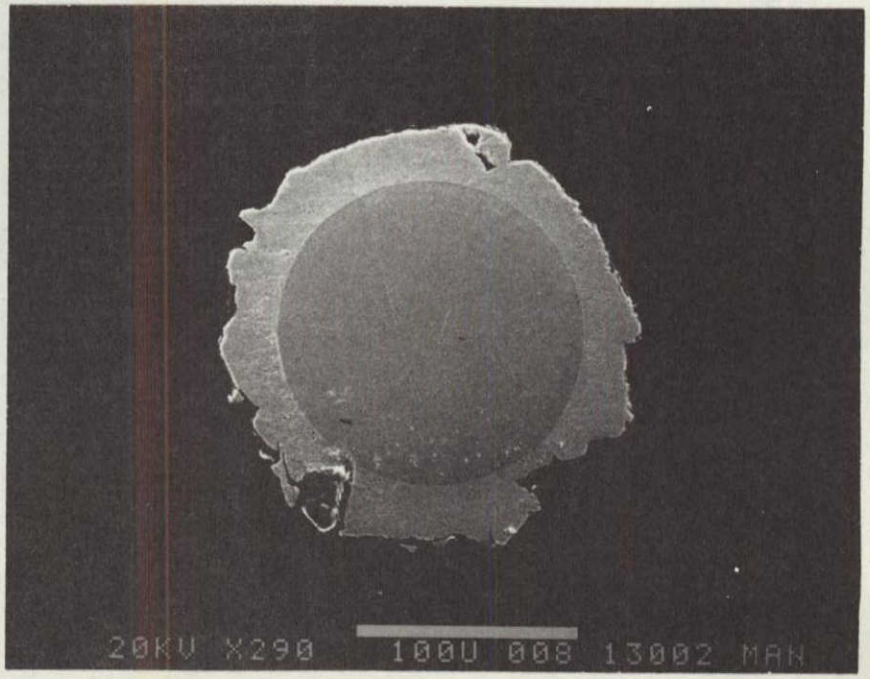

Figure 5. SEM of 8 mil, .2 mm Copper Plated Stainless Steel Wire Impregnated with 45 μm Diamond Used in Run 13 (300X and 2000X)

The blades were fabricated with a proprietary process by nickel plating 400 mesh diamonds onto a 5 mil, .13 mm stainless steel wire. SEM photographs are presented in Figure 6, SEM of 5 mil, .13 mm Stainless Steel Wire Nickel Plated with 400 Mesh Diamonds, Unused, (300X and 2000X). Note the high concentration of diamonds in relation to the impregnated wire. Swarf removal was considered essential for this high diamond concentration. Swarf could easily fill in the small spacing between diamonds. In view of this, water with no additives was flushed over the work and out the drain. This prevented the possibility of swarf build-up that occurs in the coolant during recirculation.

At a blade force of 0.15 pounds, 68 gm. per blade, cutting rates held in the vicinity of 3 mil/min, .075 mm/min, during much of the run, but wire breakage was a problem toward the end of the cut. This was apparently the result of hydrogen embrittlement during plating, related to the evolution of hydrogen. The wires were not baked at 450^{o}F as is a typical treatment for preventing hydrogen embrittlement in stainless plated products.

A wire that had cut completely through the silicon block was examined with an SEM for signs of degradation. An SEM of the used wire is presented in Figure 7, SEM

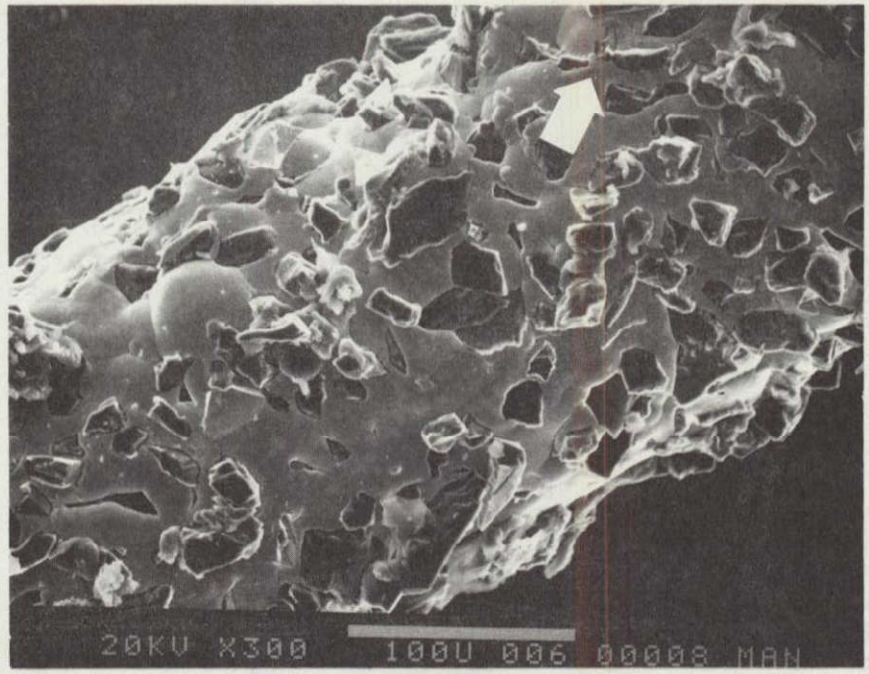

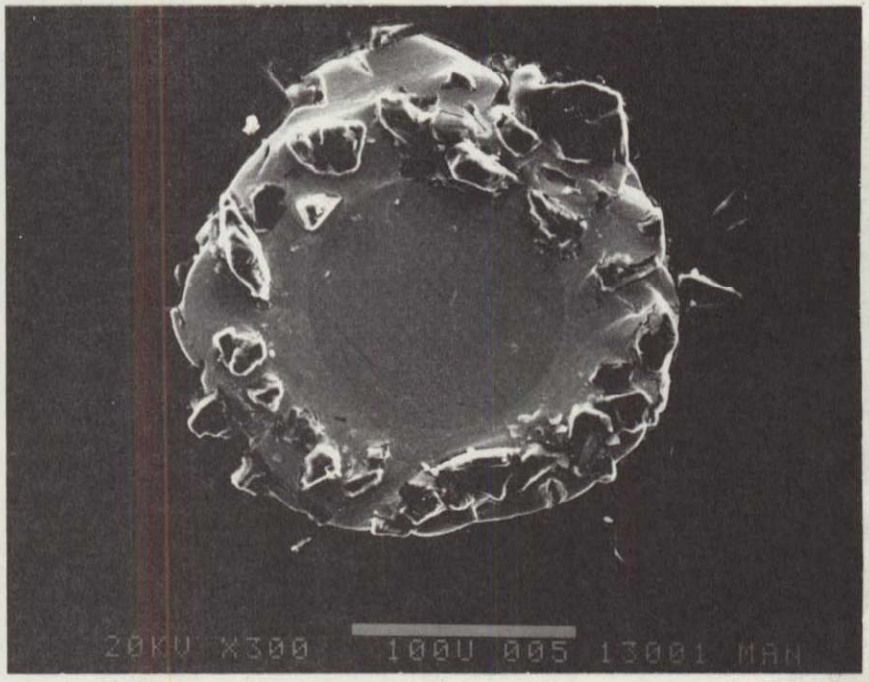

Figure 6. SEM of 5 mil, .13 mm Stainless Steel Wire Nickel Plated with 400 Mesh Diamonds, Unused (300X and 2000X)

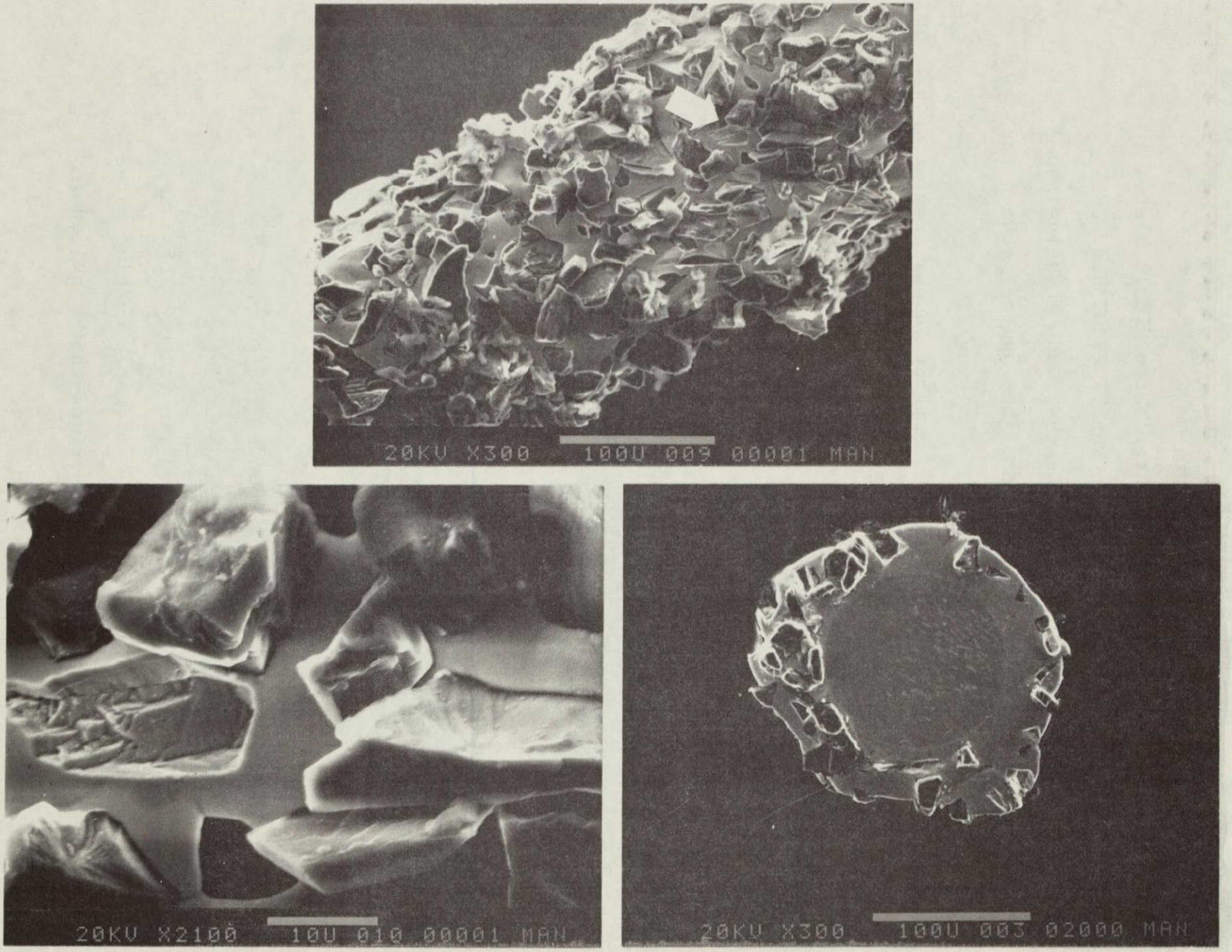

Figure 7. SEM of .5 mil, .13 mm Stainless Steel Wire Nickel Plated with 400 Mesh Diamond Used in Run 14. (300X and 2000X)

of .5 mil, .13 mm Stainless Steel Wire Nickel Plated with 400 Mesh Diamond Used in Run 14 (300X and 2000X). No signs of degradation can be observed. Loading and swarf can be observed in some of the spaces between the diamond particles.

Wafer surface texture in terms of waves, scoring, and similar visible properties appeared particularly good.

Run 15

Run 15 was a brief test of cutting dry with a single wire of the double diamond impregnated type used in runs 12 and 13. Results of the test were inconclusive, but further testing of cutting dry is anticipated.

Run 16

In run 16 the workpiece was held rigidly without rocking. Double impregnated wire blades of the type used in runs 12, 13, and 15 were used. Water was used as the coolant.

A blade force of 0.3 pounds, 136 gm. per blade was required in order to obtain cutting rates in the 2 to 3 mil/min, .05 to .075 mm/min range. This was twice the force required for comparable cutting rates in run 8 and one and one-half times that required in

run 13, runs in which the workpiece was rocked with synchronous motion and a phase angle of 90^{o}.

Cutting rates of 2 to 2.5 mil/min, .05 to .065 mm/min were maintained at first; then wires broke and cutting rates deteriorated to near zero at the end of the cut.

In addition, wafer surfaces were uniformly wavy to an unacceptable extent throughout the cut.

The run was considered verification of previously held attitudes favoring the use of small contact areas and low cutting forces for obtaining maximum cutting rates and the best wafer surface quality.

Run 17

Run 17 was intended to determine the effects on slicing performance of rocking the workpiece with a slow, non-synchronous motion.

Blades were of the double impregnated type used in runs 12, 13, 15, and 16. Water was used as a coolant and the workpiece was rocked with a frequency of one-half cycle per minute.

At a blade force of 0.2 pounds, 90 gm. per blade cutting rates were maintained in the range of 2 to 3 mil/min, .05 to .075 mm/min throughout the run.

The wafer surfaces generated in this run were

dramatically smoother in appearance than wafer surfaces from previous tests, with virtually no waves, scoring, steps or other typical surface damage.

The cut was made in one continuous operation with no shutdowns and startups. In addition, prior to the run the feed mechanism was modified slightly in order to eliminate some of the play in rocking components.

The entire wafer surfaces from this run appeared of comparable quality to the very best smaller areas on wafers from earlier runs with synchronous rocking of the workpiece at a phase angle of 90^{o}.

For slicing runs 18 through 36 a wire pack with twenty-eight 5 mil, .127 mm diameter tungsten wires was used. Tungsten was chosen as a core material because of its high modulus of 50 million and high strength 400 thousand psi. Four-hundred-mesh diamonds were electroplated on the wire with a nickel plating. SEM photographs of unused wire are presented in Figure 8, SEM of Tungsten Wire 5 mil., .127 mm Nickel Plated with 400 Mesh Diamond Unused (300X and 2000X).

The diamond appears buried beneath the nickel plating in the unused wire and the concentration is much lower than for the diamond plated stainless steel wire.

Feed forces for all runs was .2 pounds, 90 gm per wire. Slow non-synchronous rocking of the workpiece

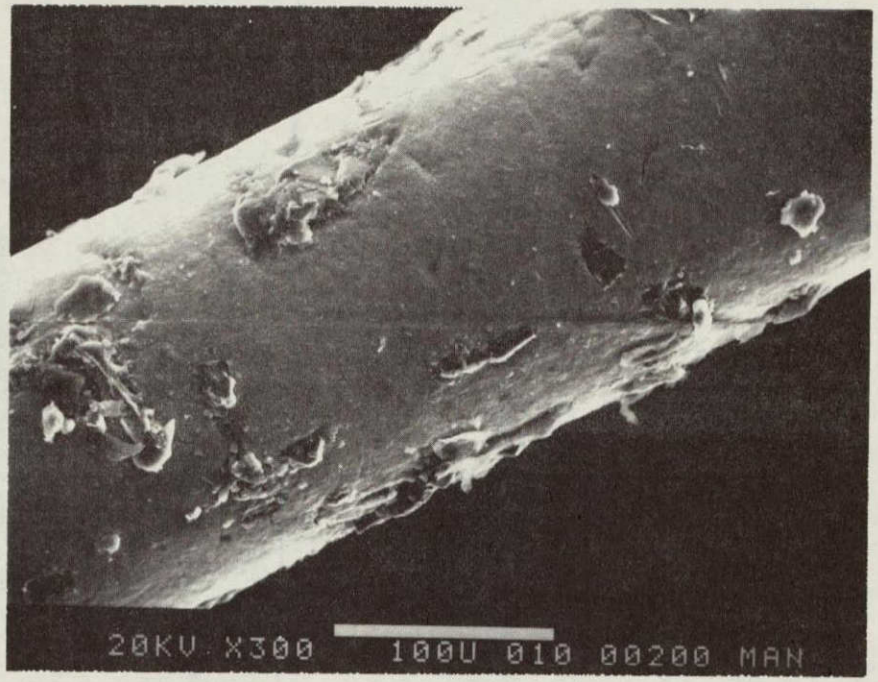

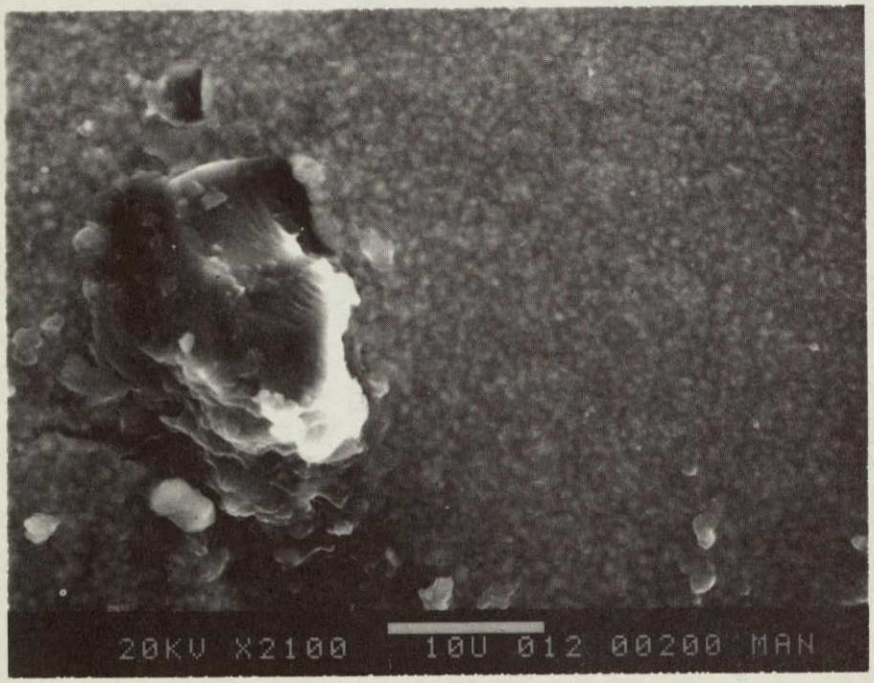

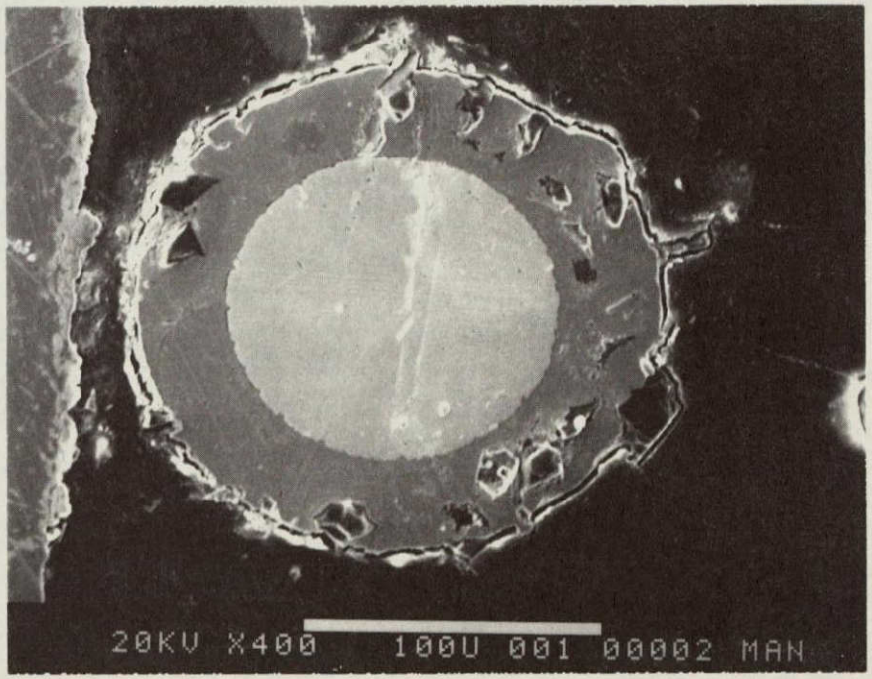

Figure 8 SEM of Tungsten Wire 5 mil, .127 mm Nickel Plated with 400 Mesh Diamond Unused (300X and 2000X)

was used for all tests.

Average cutting rates for each run are presented in Figure 9. The average rates were calculated by dividing the depth of workpiece by the length of time required to cut through it. A cutting rate of over 6 mil/min, .15 mm/min was achieved for the first run 18-S until it cut into the glass mounting block. This is illustrated in Figure 10, a graph of Cutting Rate vs. Distance Cut.

The cutting rate remained below 2 mils/min, .05 mm/min for the next run 19-S. It was terminated after cutting 2 cm and the wire package was turned over. Cutting rates of about 6 mil/min, 0.15 mm/min were experienced until the wires cut into the glass. Soaking and cleaning the wires with methanol to remove swarf or the epoxy bond did not increase cutting rates above 2 mil/min, .05 mm/min that were achieved at the end of the previous run. SEM photographs of a section of wire used in this run are presented in Figure 11, Tungsten Wire 5 mil., .127 mm Nickel Plated with 400-mesh Diamonds Used in Runs 18, 19, 20 (300X and 2000X). It appears that nickel plating has been dressed away to expose the diamonds since more diamonds are exposed than on the unused wire. No cause for the low cutting rate, such as loading or pull out, can be observed in these

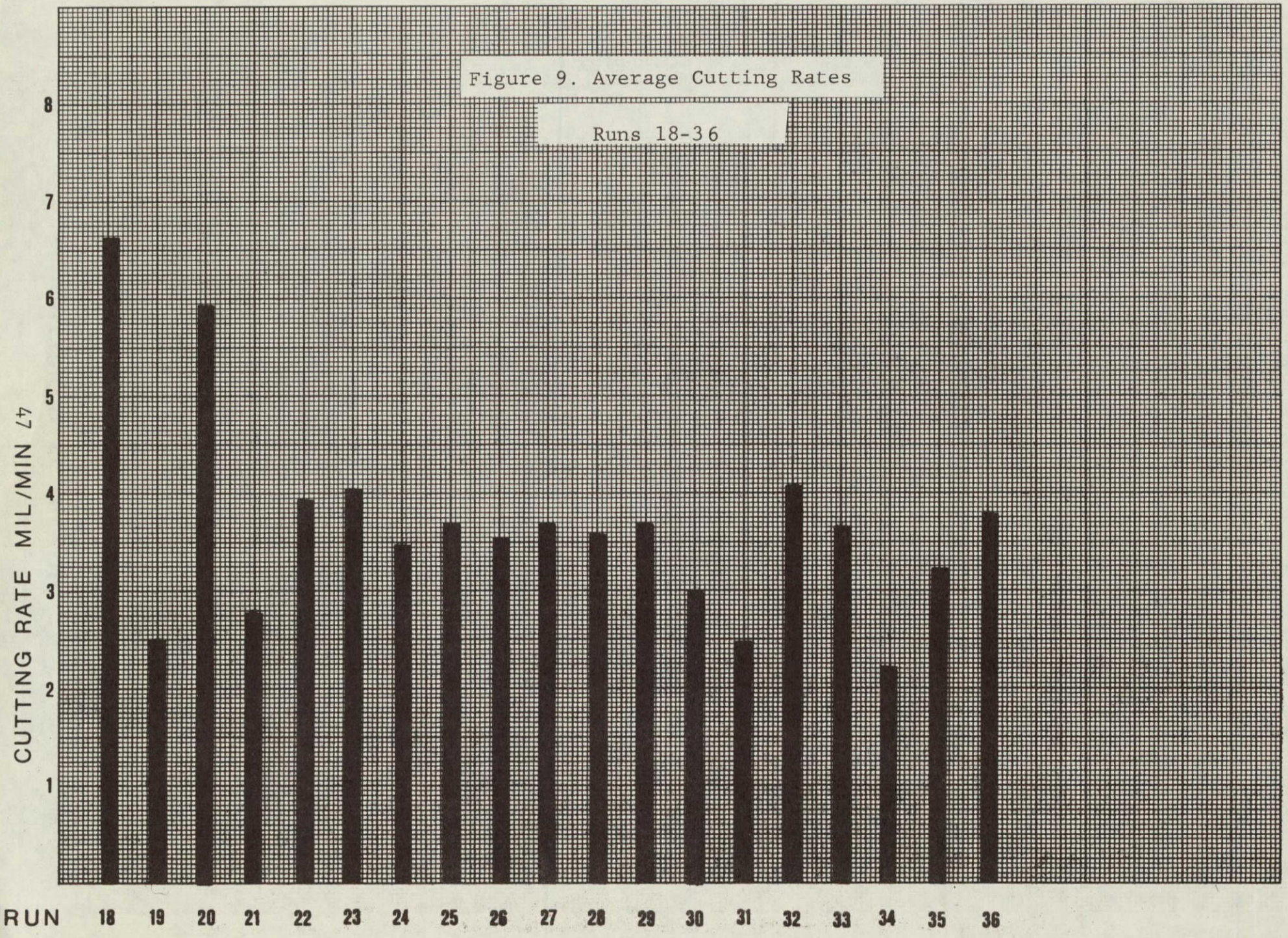
Figure 9. Average Cutting Rates
Runs 18-36
CUTTING RATE MIL/MIN
8
7
6
5
4
3
2
1
RUN
18
19
20
21
22
23
24
25
26
27
28
29
30
31
32
33
34
35
36

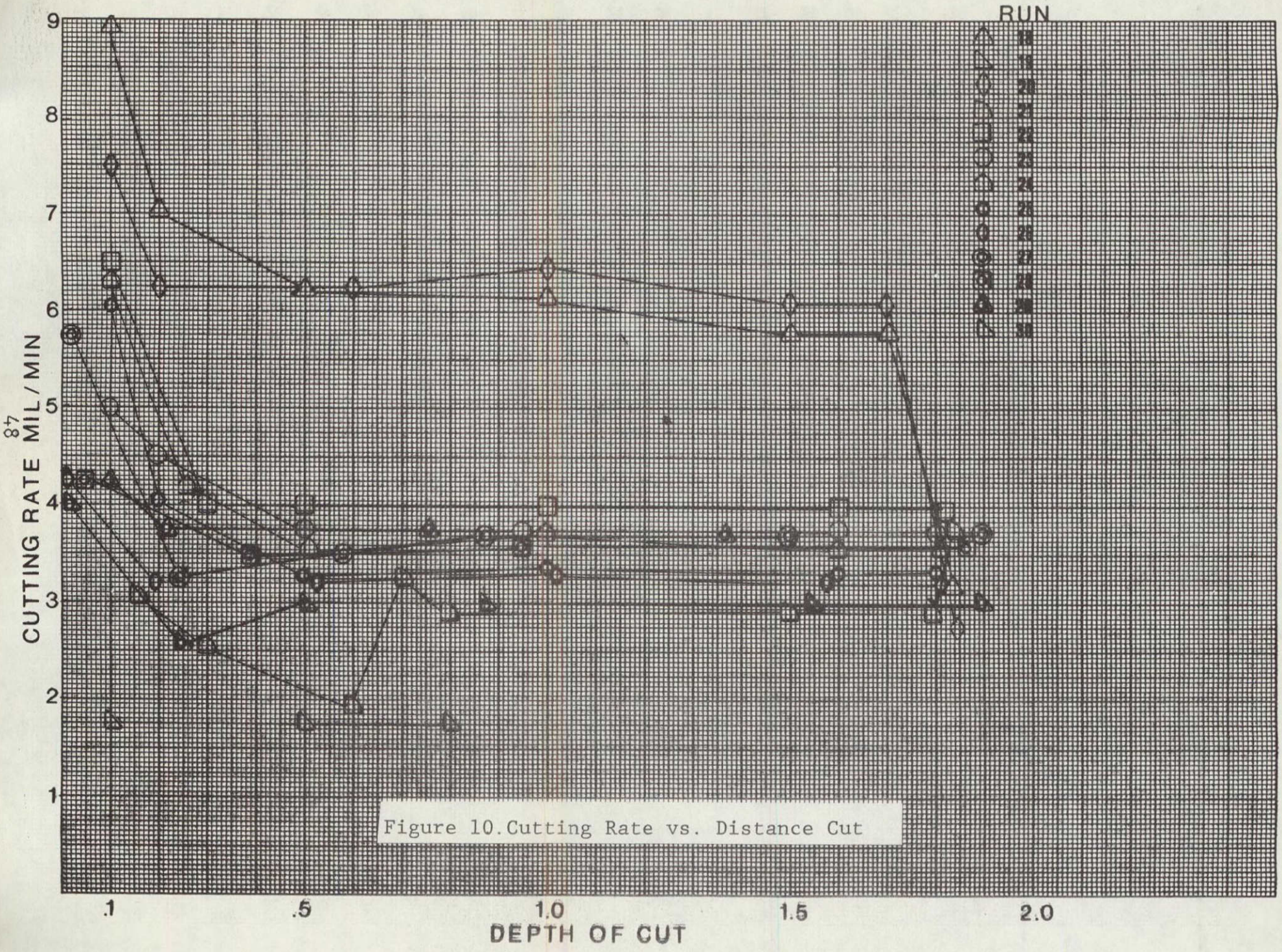

Figure 10. Cutting Rate vs. Distance Cut

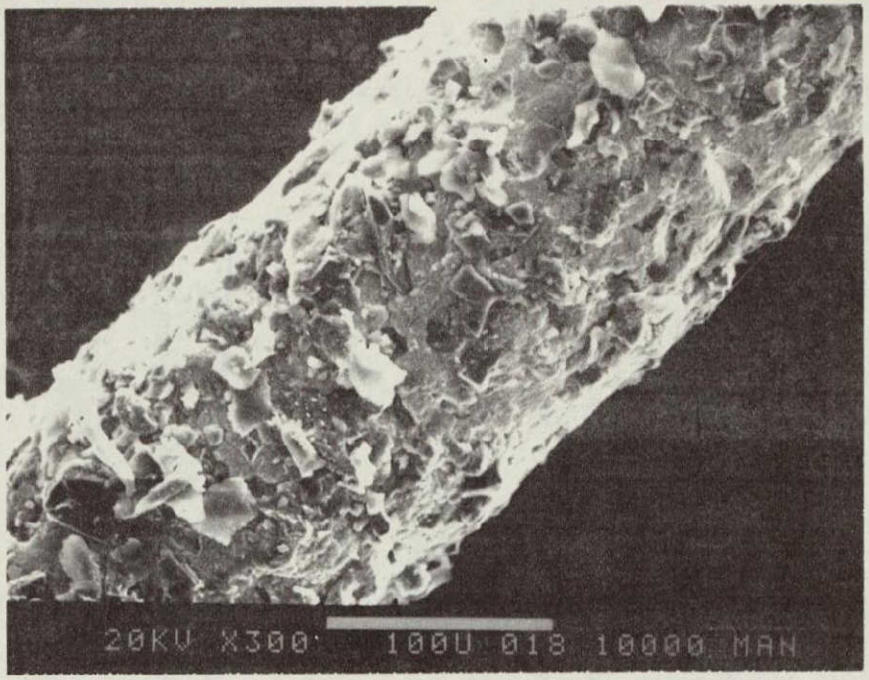

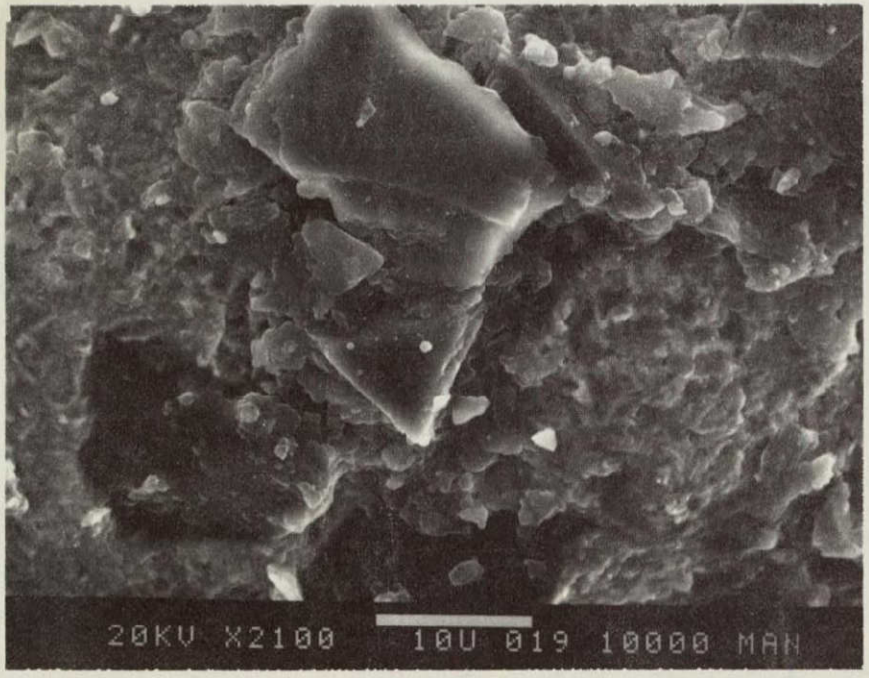

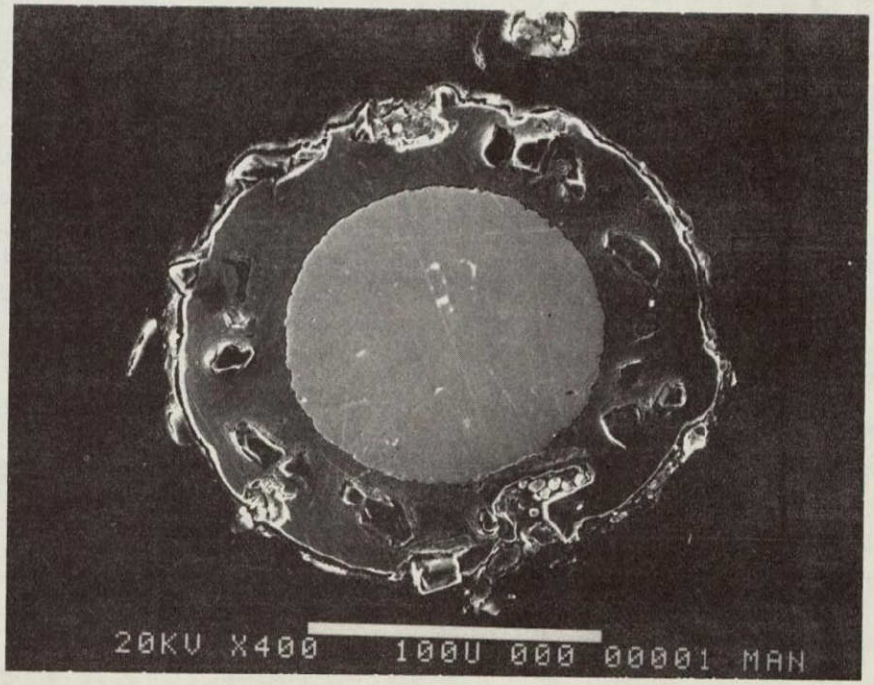

Figure 11. SEM of Tungsten Wire 5 mil, .127 mm Nickel Plated with 400-mesh Diamonds Used in Runs 18, 19, 20 (300X and 2000X)

photographs.

Light dressing with a soft Al_2O_3 stick increased the rates to 2.75 mil/min, .069 mm/min for the remainder of the run. A graphite mounting block was used rather than the glass and cutting rates increased when the wires cut into it.

For the next run 20-S, no degradation in cutting rate was experienced. An average cutting rate of 3.9 mil/min, .1 mm/min was in fact achieved after light dressing.

The glass mounting blocks that were used until this run appear to have degraded the performance and life of the wire after having cut into it. It may have turned the diamonds in their bond or caused them to become dull.

After the graphite mounting block was used, cutting rates stabilized at approximately 3.5 mil/min, .9 mm/min through run 29-S. Wafer surface quality appeared to improve for each run. Sudden increase in feed force and machine stoppage caused localized roughness increases on the wafer surfaces. The taper for the worst wafers was about 1 mil/inch, .001 mm/cm. Kerf loss was approximately 8 mil, .2 mm for all wafers. Wafer-to-wafer thickness variation increased from run 18-S to 29-S. The wires were not precision spaced in the wire

package and increasing variation in wafer thickness indicates a degradation of the grooves in the rollers.

After run 29-S the following machine modifications were performed:

1. Refinement of cylinder (feed mechanism)
2. Stiffening of vertical plate (feed mechanism)
3. More flexible hoses installed on rocking motion hydraulic system
4. Roller bearing surfaces changed to free floating to allow self-centering
5. Roller material changed to nylon instead of delrin.

Stiffening of the sensitive feed mechanism and modification of roller support system were successful as surface quality parallelism and wafer-to-wafer thickness variation in run 30-S show improvement.

Some of the noise suspected to be from the feed mechanism is in fact being transmitted through the roller support system due to acceleration of the bladehead. This condition may be minimized by altering roller support system, but this will be an inherent problem when reciprocating a massive bladehead.

For runs 31-S, 32-S, and 35-S the speed of the non-synchronous rocking was varied from one-half to 50 cycles/min. It was difficult to draw any conclusions

from these tests since the run to run differences in cutting rates outweigh the effect of changes in rocking speed. For run 35-C, the rocking rate was changed during the run. It appeared that the cutting rate increased up to about 6 cycles per minute and held constant for further increases. More conclusive results will be obtained when the number of wires is increased, since this increases the sensitivity.

Runs 33-S and 34-S were conducted to determine the effect of bladehead speed on cutting rate and surface quality. For run 34-S the entire cut was made at 40 cycles/min, half the usual speed. Cutting rates of 2.2 mil/min, .06 mm/min were maintained throughout the run. There was no observable difference in surface quality over previous runs. For run 33-S, the cutting rate increased directly with the bladehead speed, as shown by other investigation for loose abrasive slicing.

Run 36-S was conducted to determine the effect of dry cutting. The dry cutting was aborted after cutting less than a mm, due to loading of the blade. The run was continued wet with an average cutting rate of 3.76 mil/min, .1 mm/min, indicating that there was no damage to the wire from cutting dry.

After 18 runs with the same diamond-nickel-tungsten blade package, all producing the highest quality wafers

obtained from the program to date, no significant deterioration of performance had been observed. No wires or wafers have broken throughout these tests. If there was no mechanical failure of the wire, only degradation in cutting performance, the whole blade package could be turned over for further cutting.

As blade life increases, a critical analysis of wire abrasive and bond degradation is important due to the time element involved in testing to destruction.

CONCLUSIONS

1. Fast solidification rates were achieved by reducing the furnace temperature as close to the melt point as the instrumentation would allow--3°C. Good single crystal growth was achieved on top of the seed by this technique, but the periphery of the seed was too cool to seed single crystal growth.

2. Rapidly cooling ingots from 1000°C by quenching with helium did not prevent cracking of the ingot by shattering the crucible.

3. Fused silica or quartz bodies fabricated from bonded powders must be dense to prevent penetration. The wetting characteristics of liquid silicon in a vacuum atmosphere were sufficient to cause penetration into open porosity cracks or voids.

4. Grooved rollers positioned on either side of the workpiece have been effective in reducing wander to less than 1 mil/inch or 0.01 mm/cm.

5. Surface quality was dramatically improved with the use of slow, non-synchronous rocking of the workpiece.

6. Slicing a stationary workpiece required twice the blade force (0.3 lb/wire) to obtain cutting rates comparable to those measured while slicing a rocking

workpiece. This resulted in wire breakage, rapid decrease in abrasive life, and rough, wavy silicon wafer surfaces.

7. Wires fabricated by nickel plating diamond on a tungsten core have exhibited good performance for over eighteen runs. No wires or wafers have broken, and slicing performance and wafer quality have not deteriorated after eighteen cuts through 4 x 4 cm workpieces.

SCHEDULE OF MILESTONES--INGOT CASTING

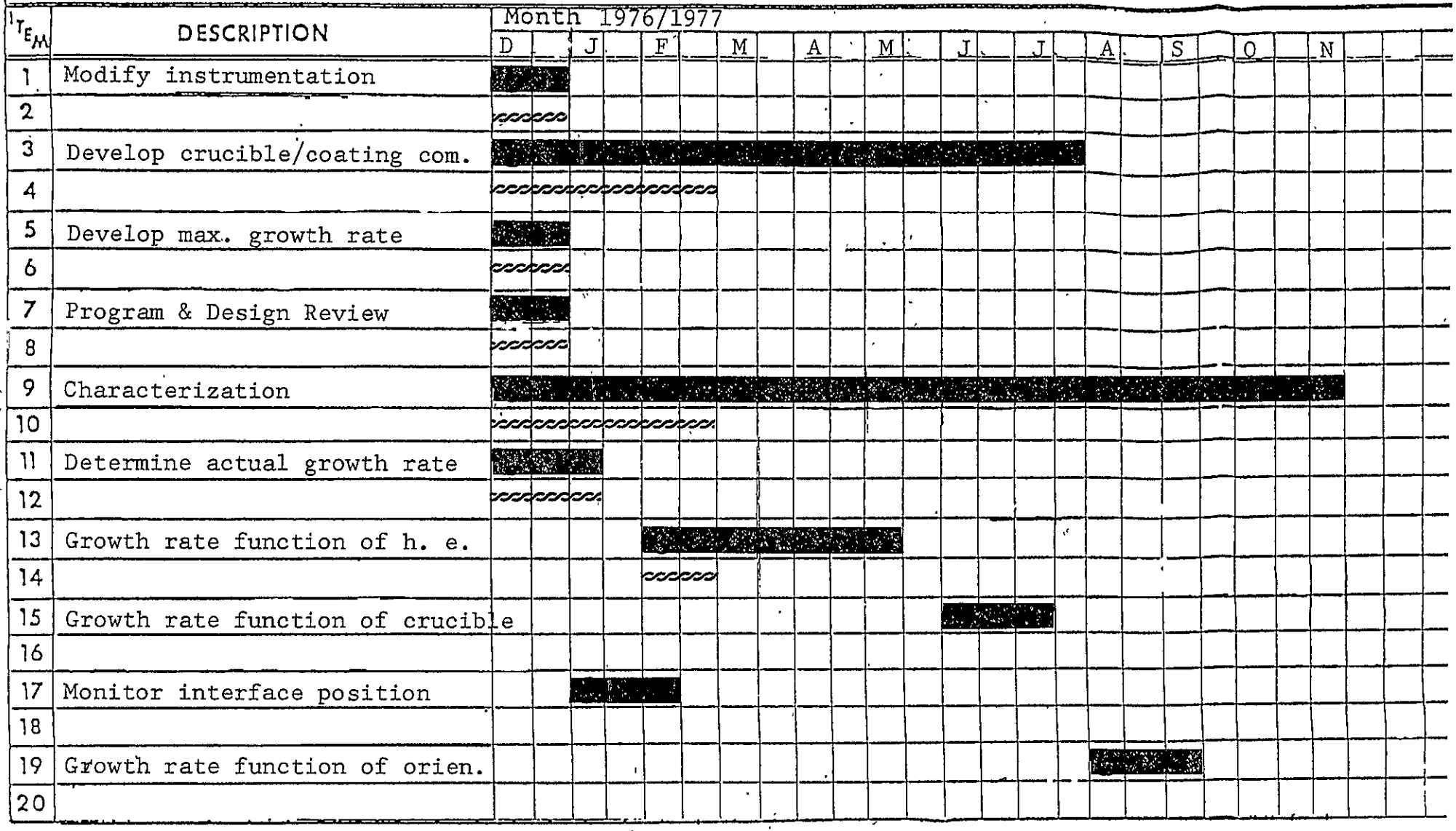

ITEM	DESCRIPTION
1	Modify instrumentation
2	
3	Develop crucible/coating com.
4	
5	Develop max. growth rate
6	
7	Program & Design Review
8	
9	Characterization
10	
11	Determine actual growth rate
12	
13	Growth rate function of h. e.
14	
15	Growth rate function of crucible
16	
17	Monitor interface position
18	
19	Growth rate function of orien.
20	

SCHEDULE OF MILESTONES--Ingot Casting

ITEM	DESCRIPTION	Month 1976/1977 D	J	F	M	A	M	J	J	A	S	O	N
1	Growth rate function of Ø									■	■		
2													
3	Draft final report												■
4													
5													
6													
7													
8													
9													
10													
11													
12													
13													
14													
15													
16													
17													
18													
19													
20													

CRYSTAL SYSTEMS, INC.
CONTRACT # 954373

SCHEDULE OF MILESTONES--INGOT SLICING

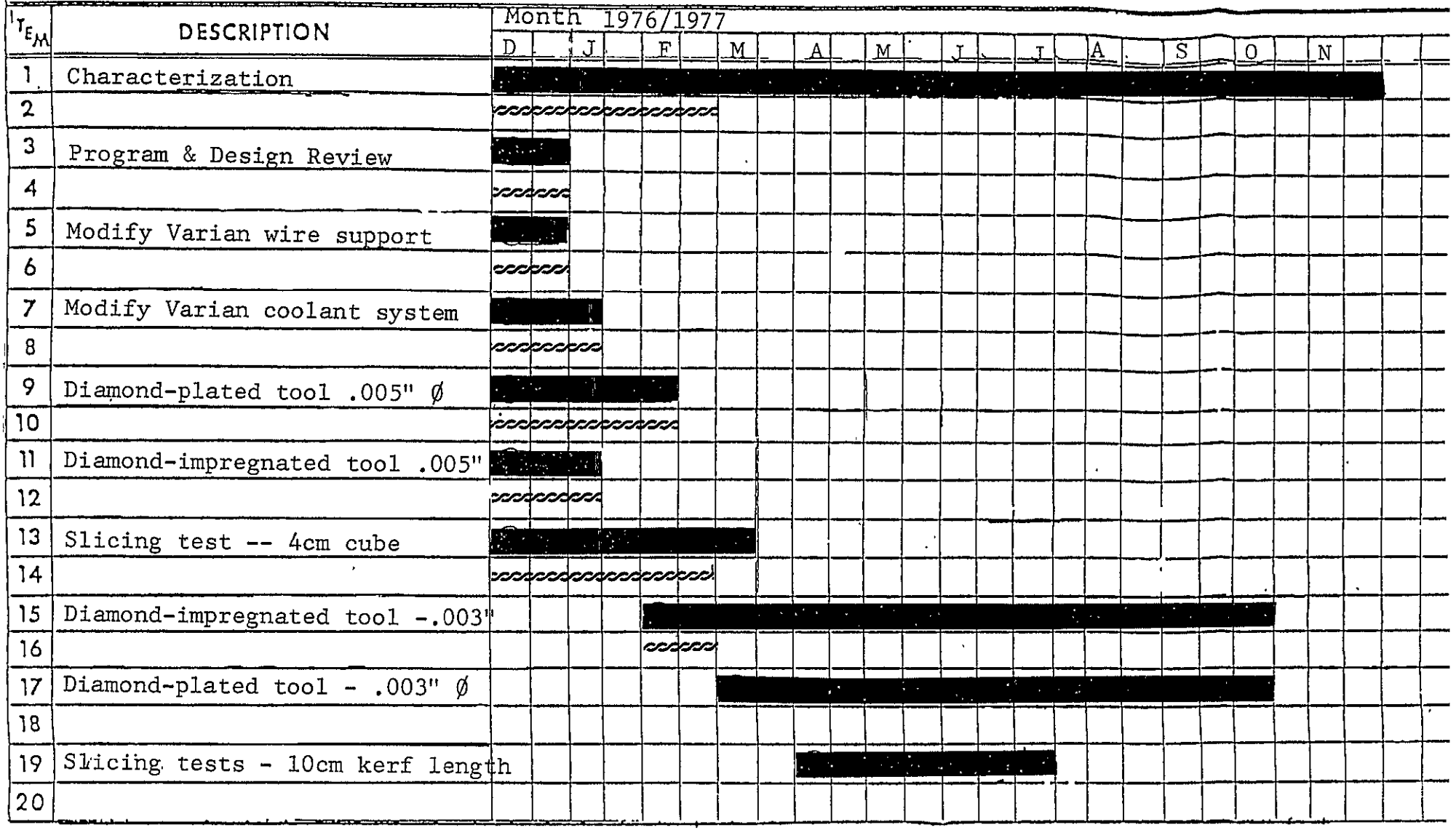

ITEM	DESCRIPTION	Month 1976/1977 D	J	F	M	A	M	J	J	A	S	O	N
1	Slicing tests - .015cm wafers									■	■		
2													
3	Slicing test-10cm x 15cm											■	
4													
5	Slicing test - .015 wafers												■
6													
7	Draft final report.												■
8													
9													
10													
11													
12													
13													
14													
15													
16													
17													
18													
19													
20													

SD

CRYSTAL SYSTEMS, INC.
CONTRACT # 954373

CRYSTAL SYSTEMS, INC.
Contract No. 954373

Sheet 1 of 2 Program: LCSSAP - Silicon Ingot Casting/Slicing Rev. Date

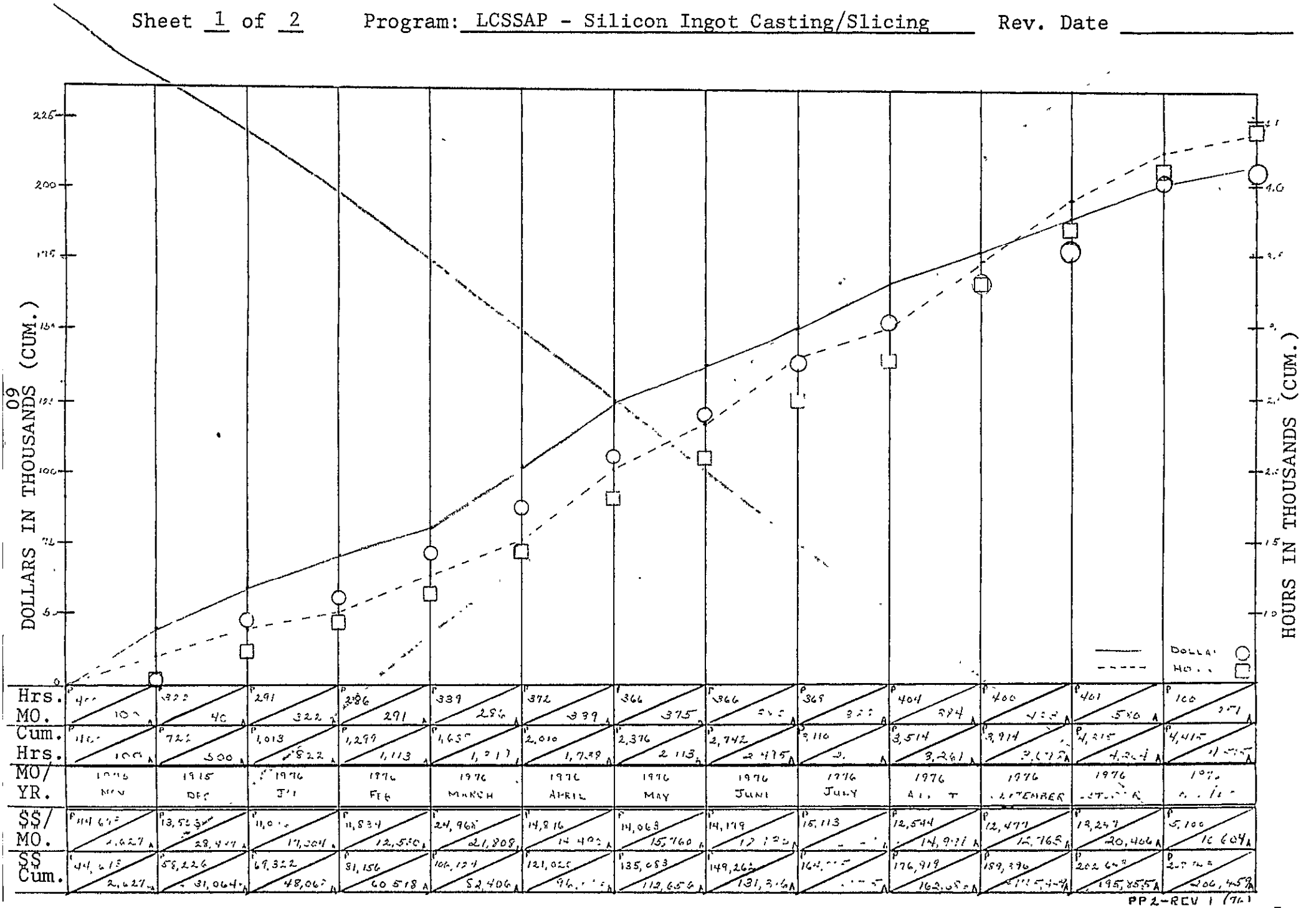

Hrs. MO.	401 / 107	322 / 40	291 / 322	286 / 291	339 / 286	372 / 339	366 / 375	366 / 375	369 / 325	404 / 324	400 / 352	461 / 560	100 / 371
Cum. Hrs.	1,107 / 1,107	721 / 500	1,013 / 822	1,299 / 1,113	1,638 / 1,452	2,010 / 1,789	2,376 / 2,113	2,742 / 2,475	3,110 / 2,800	3,514 / 3,261	3,914 / 3,613	4,375 / 4,204	4,475 / 4,575
MO/ YR.	1975 NOV	1975 DEC	1976 JAN	1976 FEB	1976 MARCH	1976 APRIL	1976 MAY	1976 JUNE	1976 JULY	1976 AUG	1976 SEPTEMBER	1976 OCTOBER	1976 NOV.
$/MO.	14,615 / 2,627	13,599 / 28,444	11,062 / 17,304	11,834 / 12,550	24,962 / 21,808	14,816 / 14,402	14,068 / 15,760	14,179 / 17,125	15,113 / [illegible]	12,544 / 14,911	12,477 / 12,765	18,249 / 20,406	5,100 / 12,604
$ Cum.	14,615 / 2,627	58,226 / 31,064	69,322 / 48,067	81,156 / 60,618	106,124 / 82,406	121,025 / 96,[illegible]	135,083 / 112,656	149,262 / 131,316	164,[illegible] / [illegible]	176,919 / 162,[illegible]	189,396 / [illegible]	202,645 / 195,855	207,745 / 208,459

PP2-REV 1 (76)

CRYSTAL SYSTEMS, INC.
Contract No. 954373

Sheet 1 of 2 Program: LCSSAP - Silicon Ingot Casting/Slicing Rev. Date

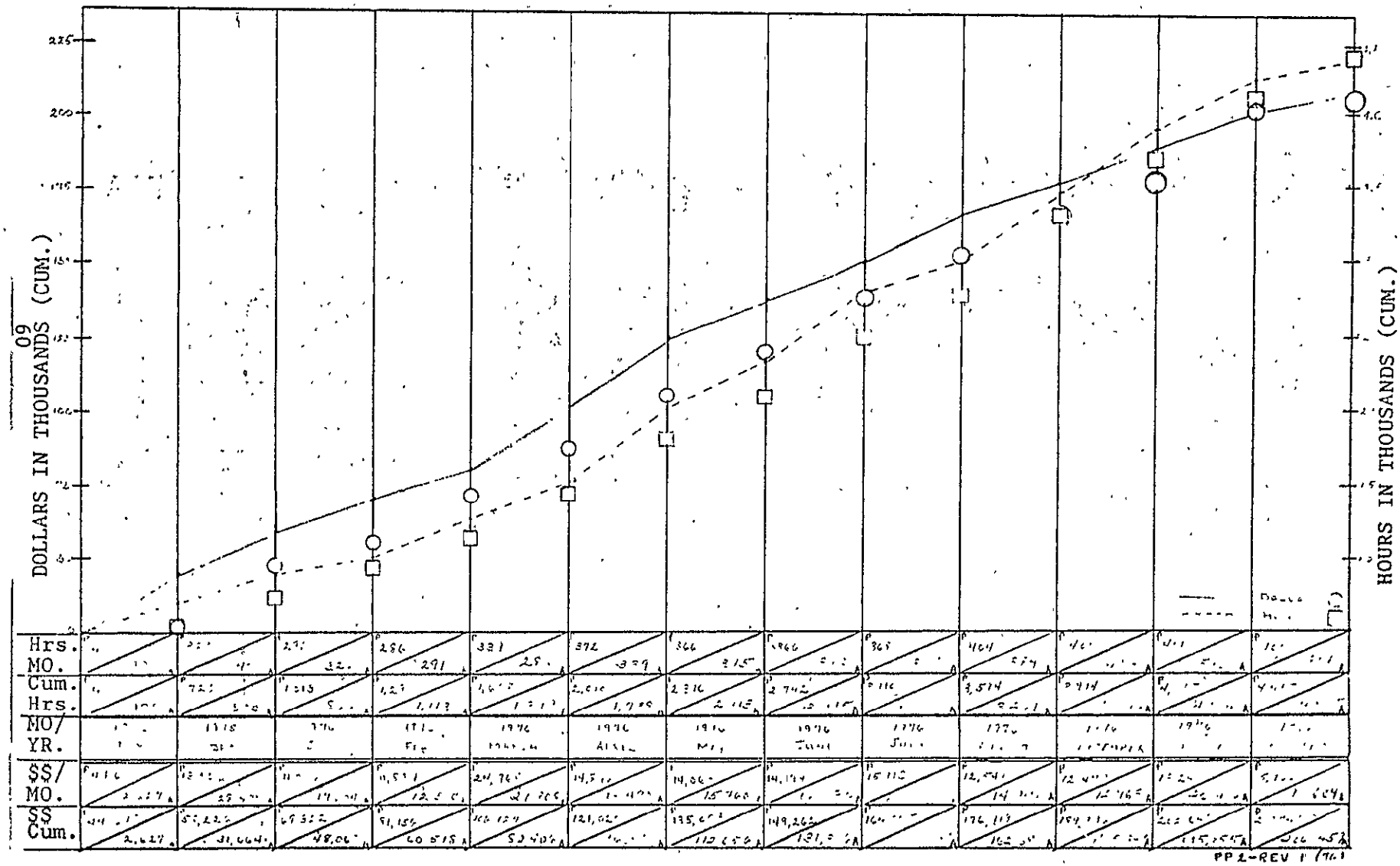

PP 2-REV 1 (76)

CRYSTAL SYSTEMS, INC.
Contract No. 954373

Sheet 2 of 2 Program: LCSSAP - Silicon Ingot Casting/Slicing Rev. Date

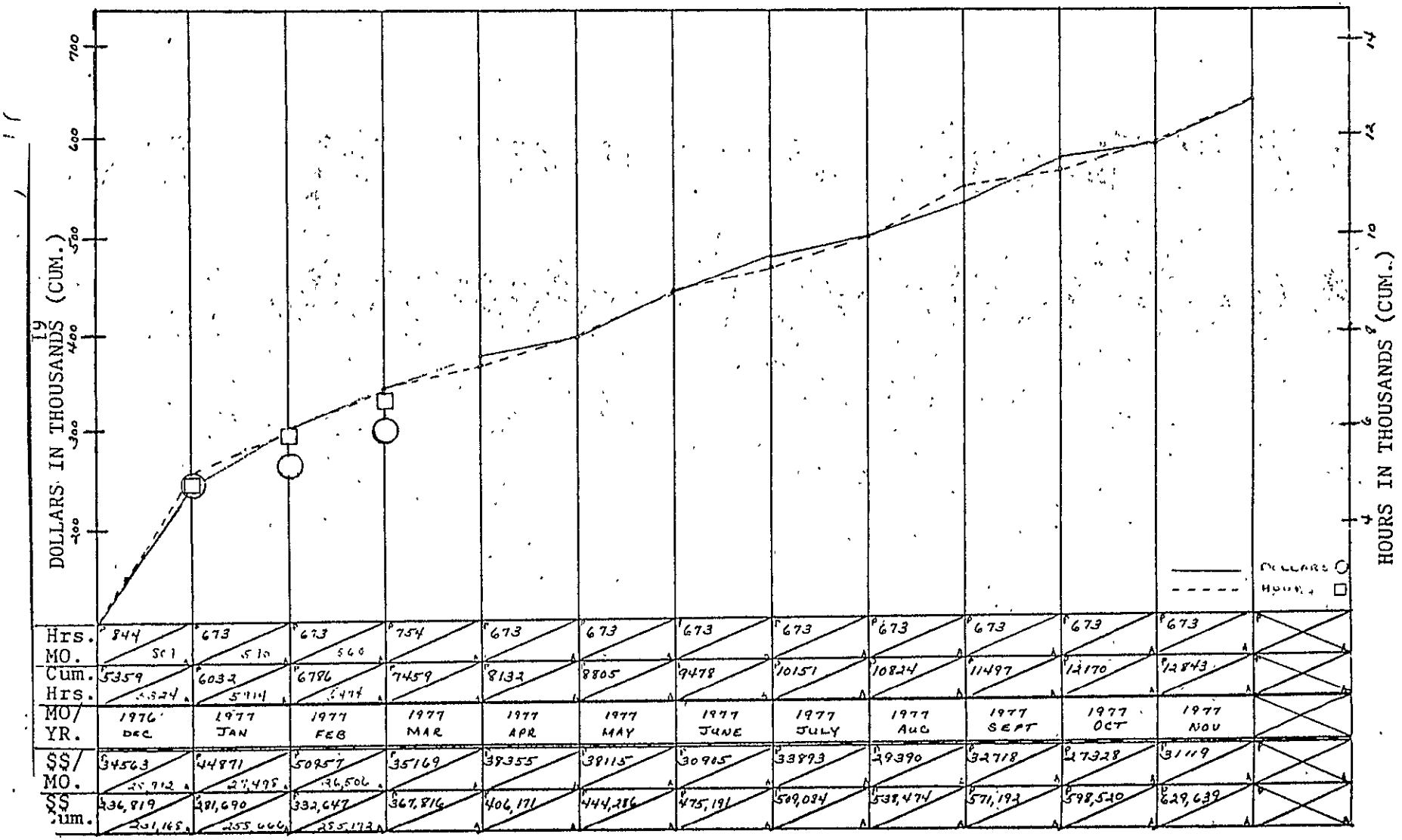

Hrs. MO.	844 / 561	673 / 510	673 / 560	754	673	673	673	673	673	673	673	673	
Cum. Hrs.	5359 / 4824	6032 / 5414	6786 / 6174	7459	8132	8805	9478	10151	10824	11497	12170	12843	
MO/ YR.	1976 DEC	1977 JAN	1977 FEB	1977 MAR	1977 APR	1977 MAY	1977 JUNE	1977 JULY	1977 AUG	1977 SEPT	1977 OCT	1977 NOV	
$$/ MO.	34563 / 25,912	44871 / 27,495	50857 / 26,506	35169	38355	38115	30965	33893	29390	32718	27328	31119	
$$ Cum.	336,819 / 231,165	381,690 / 255,660	332,647 / 255,172	367,816	406,171	444,286	475,191	509,084	538,474	571,193	598,520	629,639	